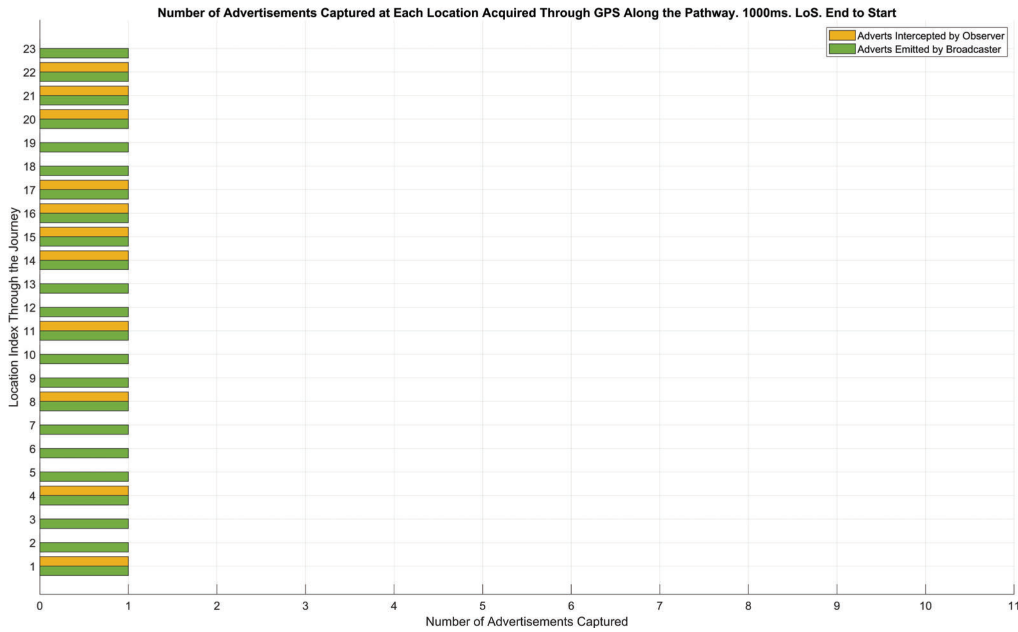


FIGURE 2.60: Advertisements Emitted vs Advertisements Captured at Each GPS Measurement for 1000 *ms* Advertisement Interval on a Walk from *End* to *Start* in LoS case

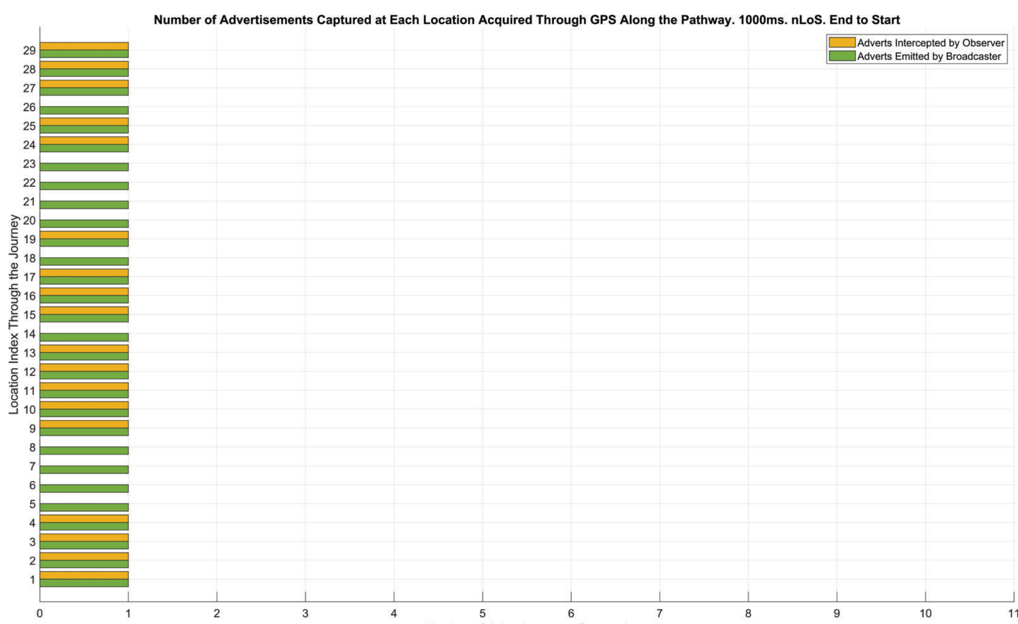


FIGURE 2.61: Advertisements Emitted vs Advertisements Captured at Each GPS Measurement for 1000 *ms* Advertisement Interval on a Walk from *End* to *Start* in nLoS case

One noteworthy observation from this experiment was that the Observer never captured more than two advertisements even when ten advertisements were broadcasted despite not restricting the sampling rate of the RPi Observer in the main Python script. This revelation hinted that either RPi and/or the Bluepy library *may* have internal restrictions on the sampling rate. This is however a speculation and more robust experimentation is required to investigate it further.

**Section Summary**

In a real-world deployment of this technology to understand pedestrians' activities, movements, and space utilisation, the Observer may be measuring data from different types of Broadcasters which may have varying advertisement rates. Therefore, this experiment is an investigation of the important parameter of advertisement interval. Three sample advertisement intervals are tested, 100 *ms*, 500 *ms*, and 1000 *ms*.

The first analysis is a simple check of the dropped advertisement interval, which presents a significantly higher drop percentage for the 100 *ms* advertisement interval, whereas the other two candidate advertisement intervals both showcase a lower drop percentage. However, this is not a very useful parameter in the real-world scenario as the advertisement interval, which is a required attribute to calculate the drop percentage, is unavailable. A crucial point to note here however is that the number of received advertisements remains similar in all the cases. This may suggest that the bottleneck is in the Observer.

When the RSSI of the advertisements are plotted against elapsed time or against the sequence number of the RSSI, a much clearer insight is obtained. While the number of advertisements captured in the case of 100 *ms* is in the same ballpark as the other two candidates, the received advertisements are spread significantly far apart. This hinders the intention of identifying patterns in the collected RSSI and subsequently, asserting associated activity or movement dynamics. The advertisement intervals of 500 *ms* and 1000 *ms* however produce similar results with the advertisements close enough to enable the identification of patterns. Another crucial yet unintended outcome of the experiment is the unravelling of the bottleneck of the Observer. When the number of advertisements broadcasted and captured are studied in figures 2.50, 2.52, 2.54, 2.56, 2.58, and 2.60, it is seen that the number of intercepted advertisements by the Observer is never more than two. This supports the inference made through the previous analysis about the limitation of the Observer used in this experiment. Note that this limitation may not apply to any other SBC apart from the one used in all the experiments conducted during this PhD.

## 2.2 Evaluation of the Platform's Abilities to Detect, Identify, and Characterise Pedestrian Movement and Activities

### 2.2.1 Pause Detection in the Movement of the Pedestrians

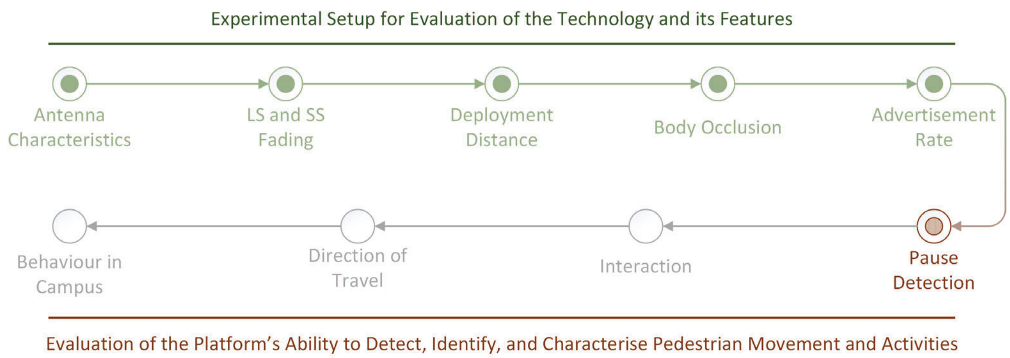


Identification of interactions with other pedestrians or the environment is simply a correlation of the pauses in the journey of a pedestrian. This approach provides no certainty that the pedestrian has paused to interact with either the surrounding environment or with other pedestrians. It is only an indication that the pause in the journey could be likely due to some form of interaction with another pedestrian or with the environment. This uncertainty is notable as it accounts for no intrusive personal behaviour monitoring and yet, if such a measurement is detected in the same region across days or with other pedestrians, it could be asserted with more confidence that the pauses are an indication of something notable or interesting in the environment or a presence, for example, of an obstruction on the path. Similarly, if two or more BLE Broadcasters pause at the same time for the same duration in the same region, it is more likely to be an interaction. But all of this information is unknown until such nuances are observed.

Measurements for this experiment were collected on June 9, 2023 between 16:51 and 17:18 hours Irish time with the support from a single volunteer pedestrian. The weather information on the day of the experiment are presented below:

**At 17:00 hours on June 9, 2023**

- **Precipitation (Rain):** 0.0 mm
- **Air Temperature:** 18.5 °C
- **Wet Bulb Temperature:** 14.2 °C
- **Dew Point Temperature:** 10.6 °C
- **Vapour Pressure:** 12.8 hPa
- **Relative Humidity:** 60 %
- **Mean Sea Level Pressure:** 1013.8 hPa

In this experiment, the interaction of the pedestrian with other pedestrians and with the environment was asserted through the identification of pauses in the movement of the pedestrian carrying a Broadcaster on the linear path. A 24-*metre* long pathway, at a deployment distance of 3 *metres* with two end points, the *start* point and the *end* point, where the former is towards the 0° region of the Observer and the latter at the 180° region was selected. A point 6 *metres* away from the *start* point was marked as the *approach* point which was a designated stop point for the volunteer pedestrian. This is depicted in Figure 1.22. In this experimental setup, three scenarios were tested with the Broadcaster always in the LoS of the Observer. First, when the pedestrian started the journey at the *start* point and paused at the *approach* point for 5 *seconds*, second, for 10 *seconds*, and finally third, for 15 *seconds*, before the pedestrian continued the onward journey to the *end* point. Each scenario was repeated four times, totalling up to 12 individual repetitions. The ground truth was obtained from the *Blue Dot* application. Collected data included the MAC address, timestamped raw RSSI and sliding window SMA filtered RSSI, and the ground truth location obtained through the use of Blue Dot.

The collected data was subjected to the analysis steps as described below:

1. *Curve Fitting*: This was performed to interpolate a smooth curve that fits the trend of measurement values of the RSSI. A polynomial equation of a selected order was applied over the measured RSSI, then curve fitting and SSE was calculated to check the closeness of the resulting curve against the actual RSSI. SSE was also used to assess the fit of curves generated with different orders of the polynomial. This two-step method is described in the Section 1.4.9 in Chapter 1. This process helped in diminishing the effect of outliers and fluctuations, and is presented as an example in Figure 2.62. As seen in the figure, the blue line and marker $\times$, representing the measured RSSI, on the $14^{th}$ sample corresponds to an anomalous dip. The effect of which are diminished in the resulting polynomial curve, in red.

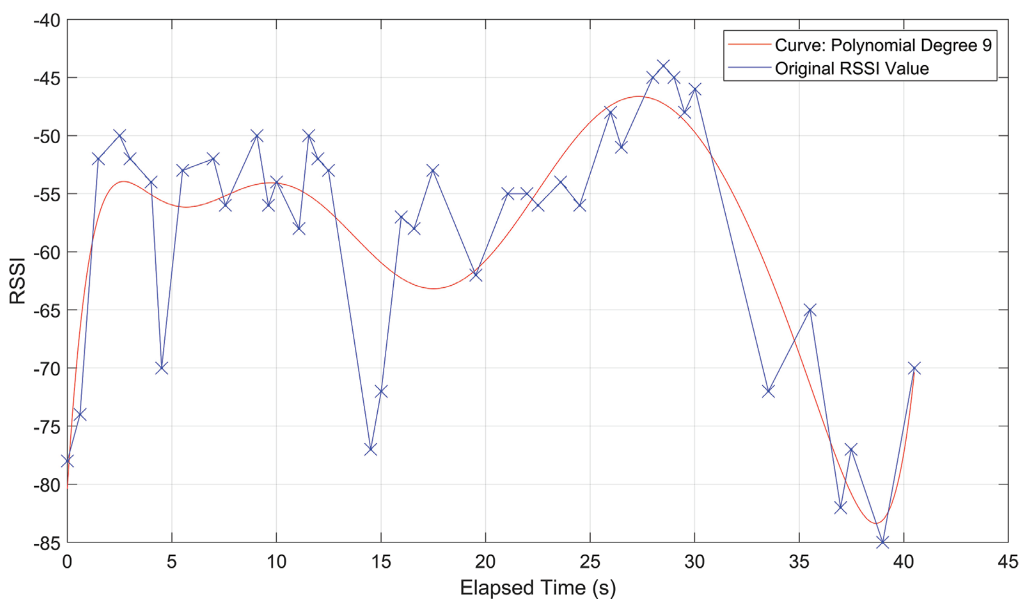


FIGURE 2.62: Curve Fitting for Example RSS Values

As mentioned in Section 1.4.9 in Chapter 1, SSE was used to identify the order of the polynomial that produces a curve that closely approximates the measurements. The order of the tested polynomials was varied from 2 to 9 for each of the four repetitions of each pause duration: 5, 15 and 25 *seconds*. A polynomial with degree 9 was selected as it demonstrated the lowest SSE, and hence approximated the measurements more closely than the other orders of the polynomial. This is shown in Figure 2.63. The curves that resulted from selected degree 9 polynomial fitting in Figure 2.64 were overlaid on the original RSS values. It is important to note that the RSS values in all the graphs presented in this experiment are interconnected using a line segment only for comprehension. There is no certainty that the same line segment would be observed if there were additional RSS values obtained between the two measured consecutive RSS values.

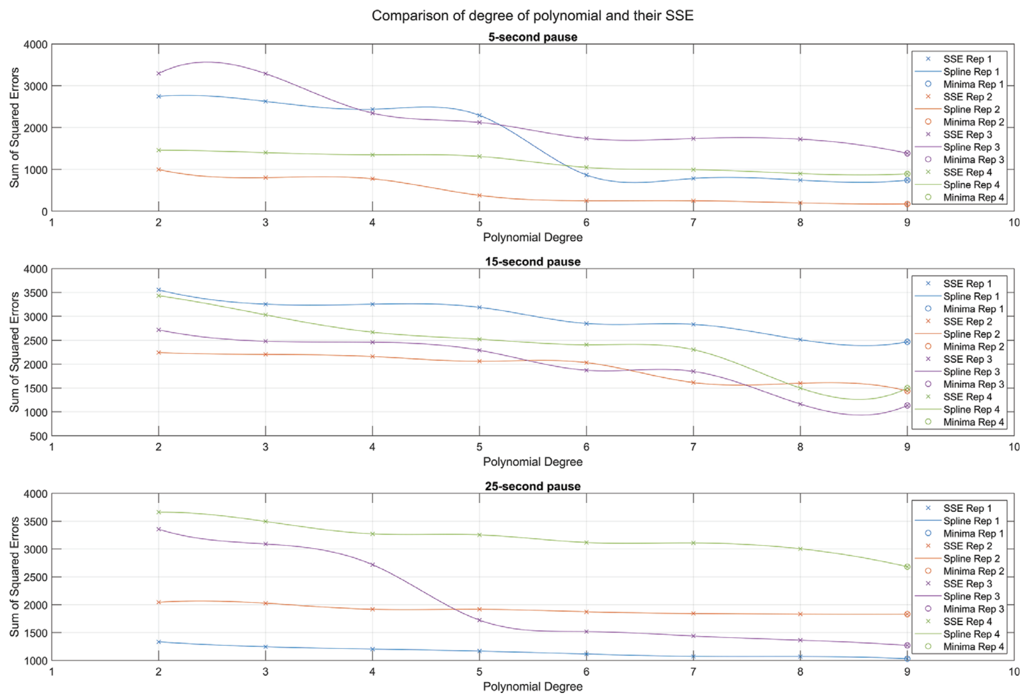


FIGURE 2.63: Comparison of SSE of Varying Degrees of Polynomial for Curve Fitting

2. *Sliding Window SD*: A sliding window on the output curve of the polynomial curve fitting was used to calculate the SD. Through this, of temporal changes in the trend of RSS values were observed. This sliding window was based on time rather than number of samples, as described in detail in the Subsection 1.4.4 in Chapter 1. As an example, a window size of 4 denotes a window of 4 *seconds* and all the data within this segment is used to calculate the SD. The choice of time-based windows ensured that no information was lost from the collected RSSI. Consideration of a time-dependent versus sample-dependent sliding window was significant as it highlights another important relevant aspect. To understand this aspect, one can observe the Advertisements from the perspective of both the Broadcaster and the Observer. Through the lens of the Broadcaster, RSS values ensuing from advertisements are regularly emitted time-series measurements since the advertisement interval for the Broadcaster used in this experiment has a fixed interval of 0.5 *seconds*. However, during transmission, as discussed in the previously in Section 2.1.4 of this chapter, these advertisements are sometimes lost or delayed, resulting in irregularly sampled time-series data from the Observer's point-of-view. If a graph of the RSS data as detected by the Observer without considering their time of detection at the top of the BLE stack was to be observed, the RSS values would appear to be evenly distributed, therefore losing the important information

about the gap in the time of arrival of two consecutive RSSI values. If the sliding window approach uses a sample-based window instead of a time-based one, it will consider the values that may be outside a trend in the overall RSSI if there are lost advertisements in between. This is depicted in Figure 2.65. Hence, to retain these nuances, a time-based windowing approach to draw inferences was adopted.

The sliding window started at the very first recorded RSS value in the entire

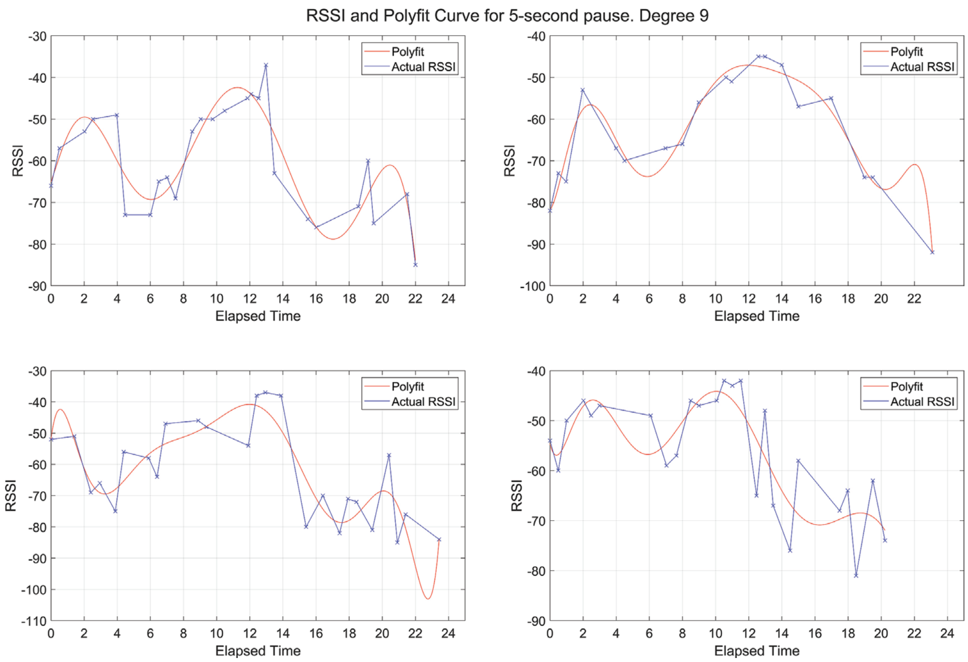


(A) 5 *Seconds* Pause All Cases

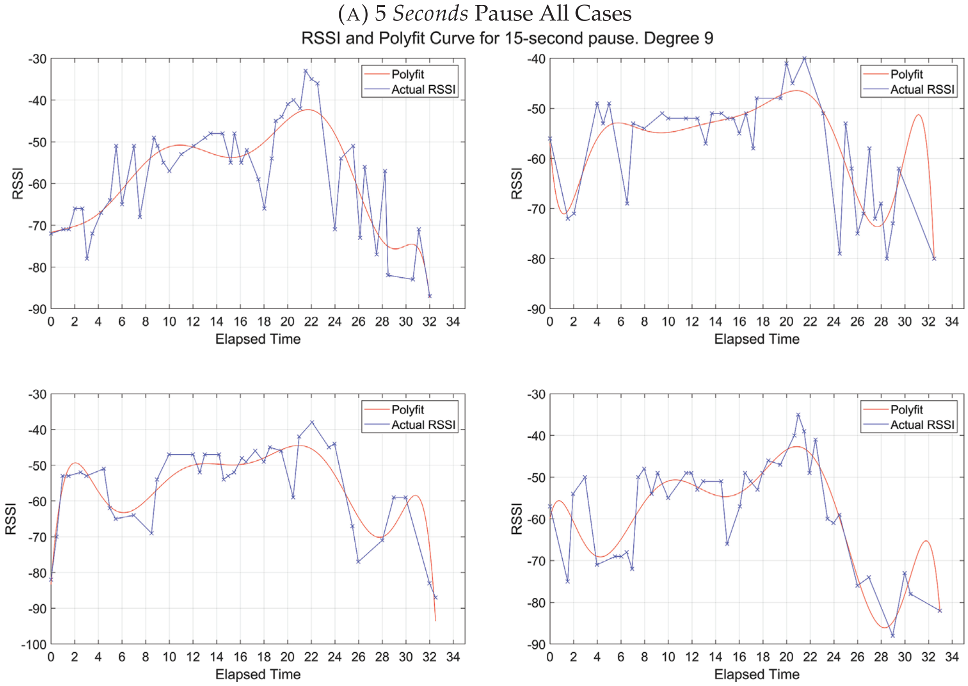


(B) 15 *Seconds* Pause All Cases

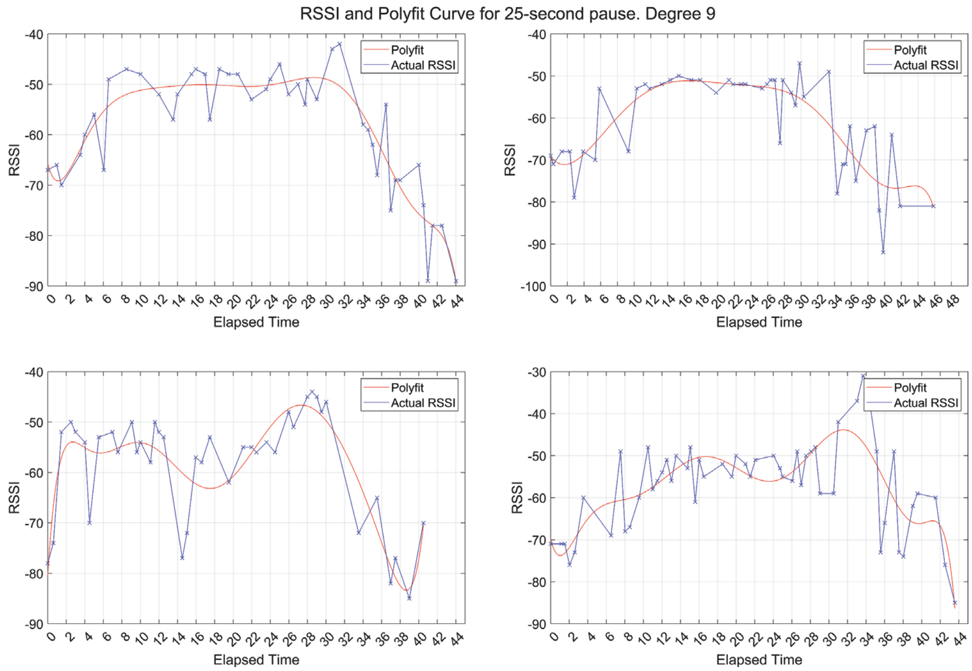


(C) 25 *Seconds* Pause All Cases

FIGURE 2.64: Polynomial Curve Overlaid on the Original RSSI

journey and depending on the size of the window, all RSSI records between the first record and the window size were converted in to a set. The window was then incremented with a step of 1 *second* to form subsequent sets until, the window was moved as far in the RSSI records that the final RSSI record is a part of the last set. SD was then computed on the RSSI records for each of those sets..

Each of the 4 repetitions from every pause duration of 5, 15 and 25 *seconds* was subjected to the sliding window subset generation that varied between 2 and 10-*second* window sizes, totalling 108 sets for the calculations of SD. Any flatness in the plot of standard deviation indicated that the RSSI did not vary significantly during that period. Since the RSSI is a function of the distance between the Observer and Broadcaster, the near constancy of the RSSI should signify a stop in the movement of the pedestrian.

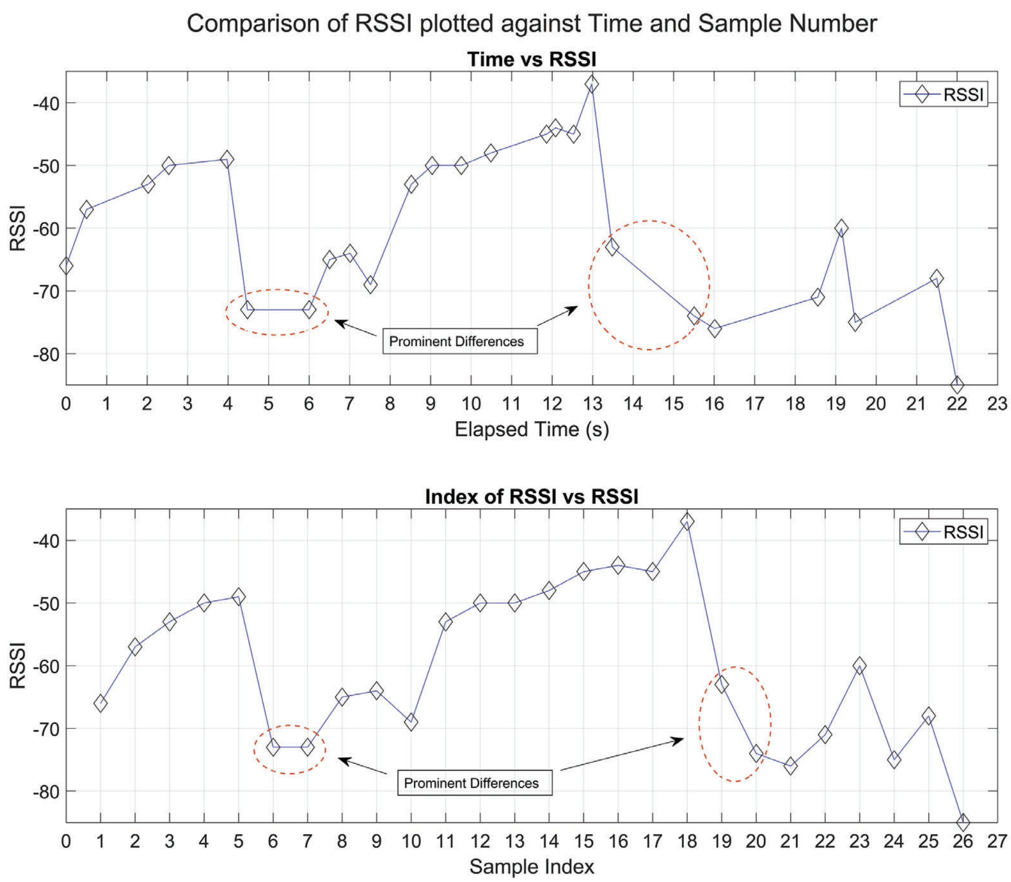


FIGURE 2.65: Curve Fitting for Example RSS Values

3. *Pause Detection and Fine Tuning* Pause detection through examination of RSS values employed a simple threshold function. Any value of SD that fell below the threshold was accepted as a pause, as seen in Equation 2.2.

$$P_n = \begin{cases} true & if SD_n < thresh \\ false & if SD_n \geq thresh \end{cases} \tag{2.2}$$

Fine-tuning of detection was performed by calculating the duration of each detected pause. If the detected pause duration was less than 3 *seconds*, it was eliminated from the detected pauses. The elimination of pauses shorter than 3 *seconds* prevented the effect of any remnant of anomalous data in the interpolated polynomial curve from causing false positives. Each of the 108 sets of SD was tested to check the number of correct pause detections and false positive pause detections for each given sliding window size, varying from 2 *seconds* to 10 *seconds*. The outcomes of that process are presented in Figure 2.66. The coloured lines represent the size of the sliding window. Each line connects to the number of false positives identified and the correct pause detection with that chosen sliding window size.

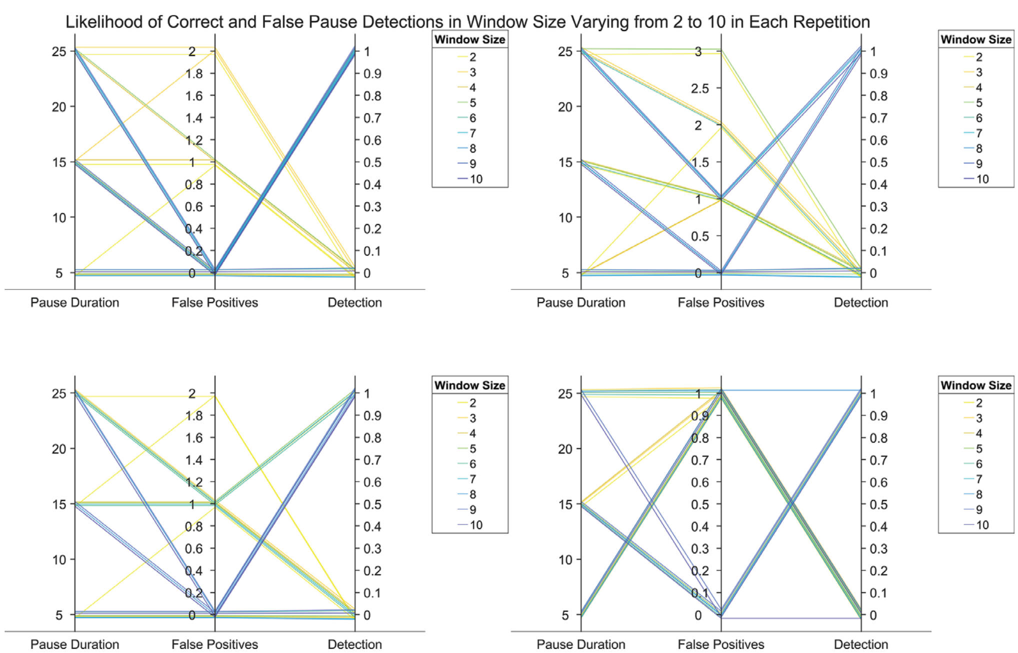


FIGURE 2.66: Sliding Window Size Efficacy Through Parallel Coordinate Plot

To select the optimum size of the window, counts of false positives and correct detection were analysed for each window size. The window size that presented the least false positives and correct detection for the most number of runs is selected. A chart depicting both the false and correct detections is presented in Figure 2.67.

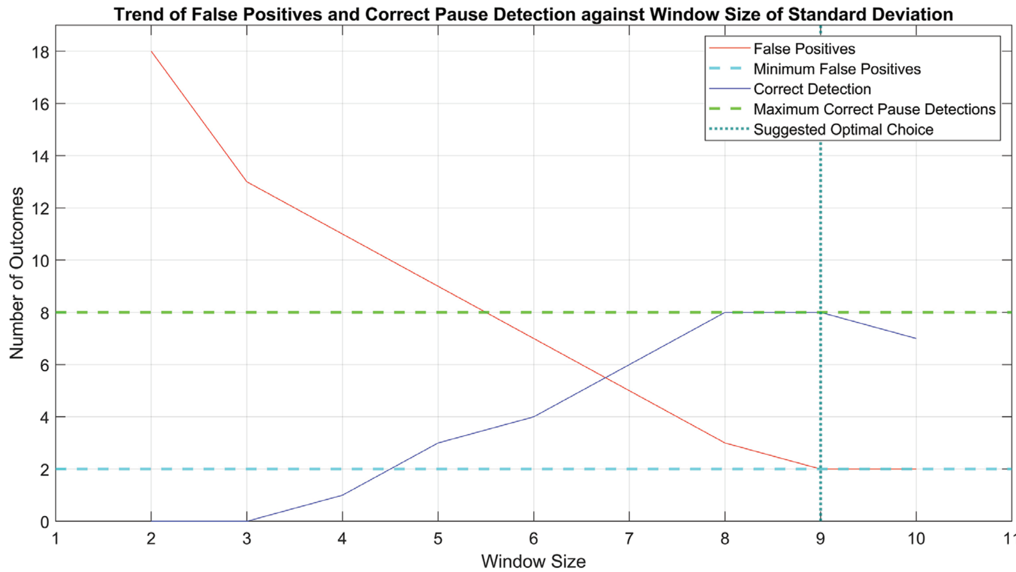


FIGURE 2.67: Curve Fitting for Example RSS Values

In this case, a sliding window with a size of 9 *seconds* provided the best balance between the two conflicting outcomes. Therefore, the final results were verified by plotting the elapsed time against RSSI overlaid with the period marked where the 9-*second* sliding window SD detected flatness.

4. *Ground Truth*: To validate whether the pause detected by our technique coincided with the point in time that the pause actually occurred, the timestamp of the button the volunteer pedestrian pressed on the *Blue Dot* app was used to confirm the volunteer's pause and the resumption of their journey. These pauses are marked on the final graph obtained from the previous step to validate if the pause detected by the algorithm coincides with the actual pause of the pedestrian. This is depicted in Figure 2.68.

With a window size of 9 *seconds*, the highest rate of detection of pauses was observed, in 8 out of 12 cases. For this window size, the lowest number of false pause detections were also observed. It is essential to note that even if many patches of below threshold SD values were identified within the actual pause duration, only one correct pause detection was added to the tally since the actual pause happened only once. All the instances of false pause detection were added up in the final tally. This further highlighted that the analytical approach resulted in a low number of false positive detections for this experimental setup.

It is also important to note that a pause was not detected at all when the pedestrian was instructed to stop for 5 *seconds*. This could be due to the stray signals from before the pause happened, overlapping the signals obtained during the pause. And since, the fine-tuning ruled out any pause length of less than 3 *seconds* duration, it was difficult to identify a pause duration this short. For a 15-*second* pause, a 100% pause detection and 0 false detections for a window size of both 8 and 9 were observed. Therefore, a recommendation of detecting a pause duration of 15 seconds or over is suggested by this experiment.

This approach indicates that it cannot be used to accurately detect pauses of less than 15 *seconds* duration, at least for the experimental configuration used in the presented experiment. Its general applicability assessment requires further investigation. This is also in line with the "smudging" effect outlined in the literature review due to fading in WiFi. Since the two technologies operate in the same radio frequency band, BLE is also prone to this effect, however, the high transmission power of WiFi makes it more susceptible to multipath fading in comparison to BLE.

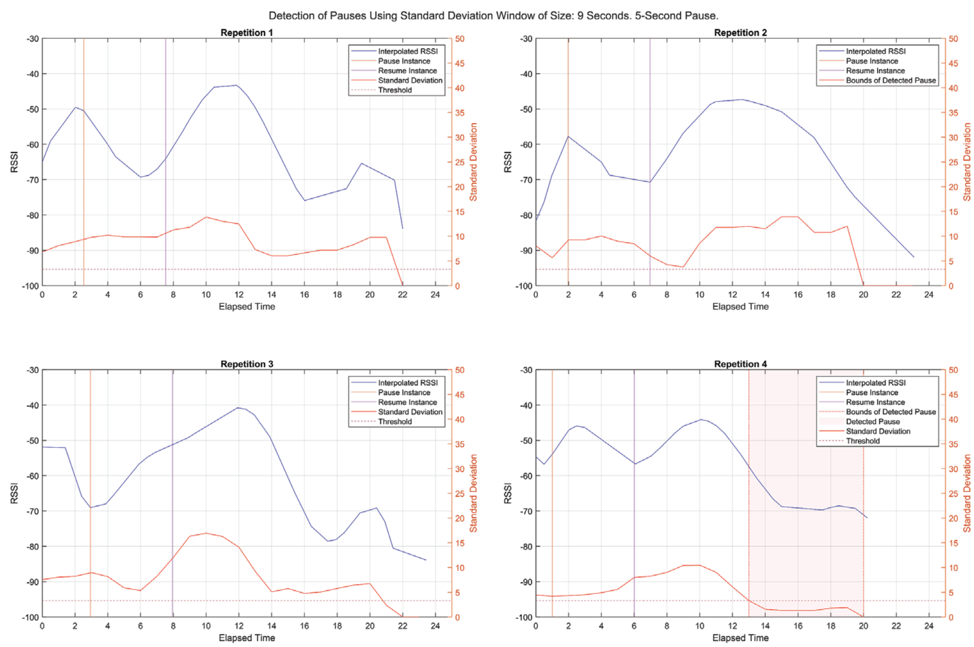


(A) Detection in 5 *Seconds* Pause, All Cases

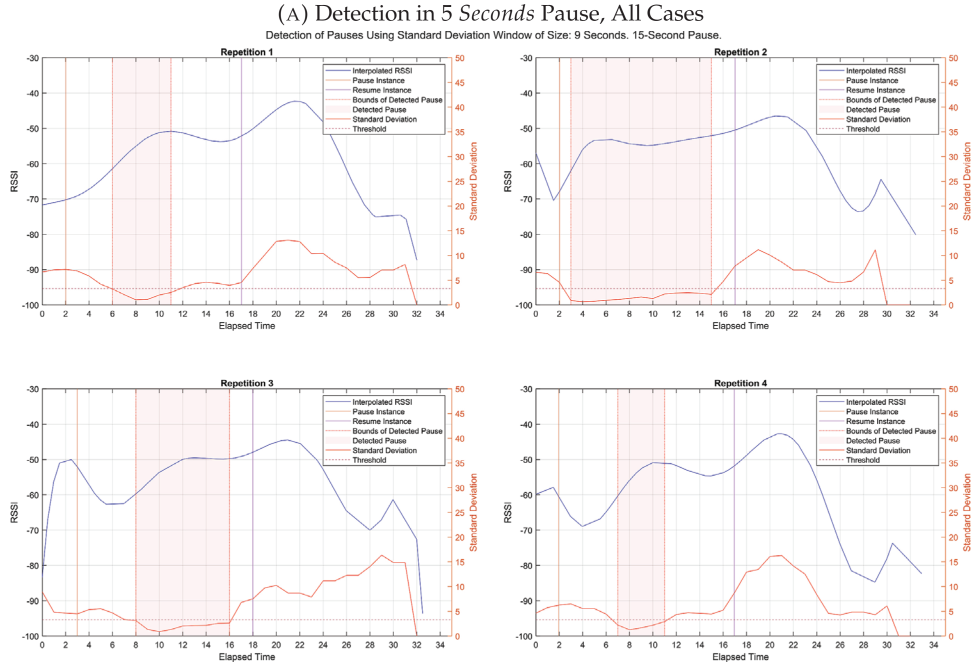


(B) Detection in 15 *Seconds* Pause, All Cases

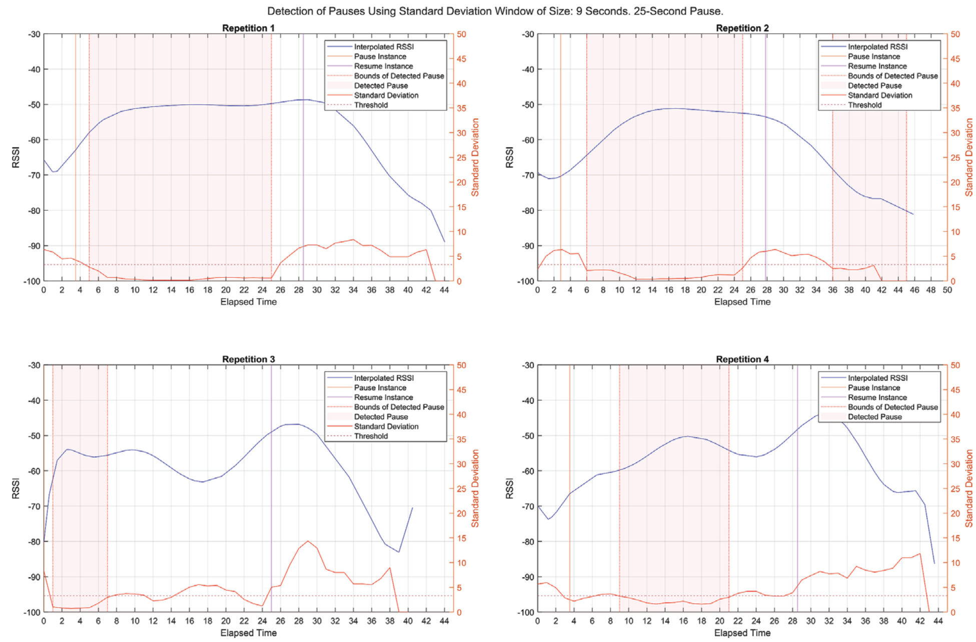


(C) Detection in 25 *Seconds* Pause, All Cases

FIGURE 2.68: Final Outcome of the Pause Detection Technique

One limitation of this approach is that there is no surety of pause detection, even at a greater pause duration. Elements present in the physical environment may amplify the reflection of radio signals and/or multipath propagation which may lead to an increased number of stray signals or repeated broadcasts reception. Therefore, a survey of the environment is essential before using this technique. Also, using polynomial curve estimation is a technique that requires further investigation. Identifying the best fit in estimated curves requires thorough research to prevent overfit and underfit, especially when the RSS values are obtained for an extended period. It should be emphasised that while a lower SSE indicates a better fit, closely aligning the curve to every data point may be ineffective in mitigating the effect of anomalous data on the RSSI trend. Additionally, the curves obtained through polynomial fitting consistently commence and conclude at the initial and final RSS values, respectively. Consequently, when there is a substantial time gap and a significant difference between the starting and ending RSS values and their adjacent RSS values, the resulting interpolated curve introduces artefacts that deviate from the actual trend exhibited by the RSS values as seen in Figure 2.64.

**Section Summary**

The results provide concrete evidence for the possibility of identifying pauses in the movement of the pedestrians. This can be associated with the interaction of the pedestrian with the environment or with other pedestrians. A multi-fold analysis is carried out to detect pauses. A curve is first fitted to the collected RSSI, for which, a variety of degrees of polynomials are tested. Once a fitting polynomial is identified, that is a polynomial that results in the least SSE, a sliding window SD is applied. For the sliding window SD, different window sizes are first tested. The optimal window size is chosen through those tests. Subsequently, a threshold on the evaluated SDs is applied to identify pauses. Finally, the duration of identified pauses is again subjected to a threshold to determine a pause in the movement of a pedestrian.

The approach however is not sufficiently robust to identify shorter pauses in the duration, as seen in the results. Therefore, detection of pauses of 15 *seconds* and over is recommended. Shorter pauses may not actually attribute to significant interaction with the space or other pedestrians regardless, and therefore, the inability of this approach to detect shorter pauses is not unfavourable because shorter pauses could mean that the pedestrian has stopped for some trivial reasons, such as tying their shoelaces or picking up something that fell or simply, the result of a set of anomalous readings. This study can be further extended with multiple BLE devices to detect whether two devices pause in the vicinity at the same time for the same duration. Such information would increase confidence in the assertion that the pedestrians could be interacting with each other.

The work described in this section is presented in a paper titled, "Detection of Pause in a Pedestrian's Movement on a Linear Walkway using Bluetooth Low Energy Received Signal Strength Indicator" (Parmar, Kelly, and Berry, 2023a).

### 2.2.2 Identifying Interactions with Other Pedestrians or the Environment

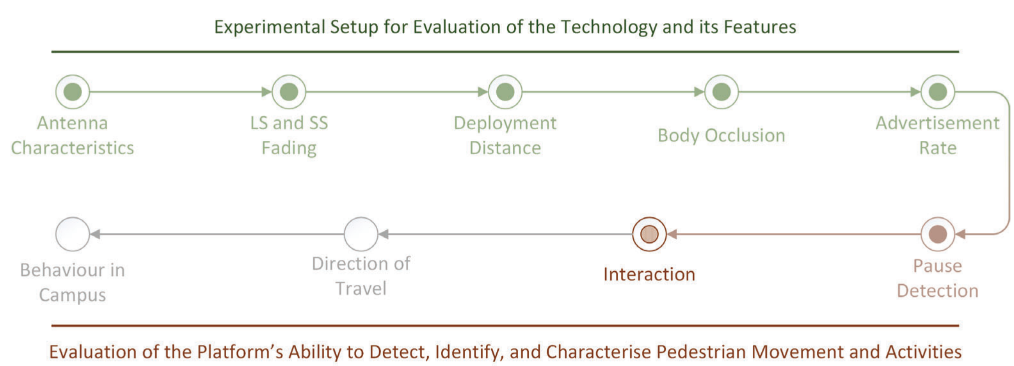


This experiment is an extension of the previous experiment 2.2.1. In the previous experiment, a pause in the movement of one pedestrian is asserted with a multi-fold analysis encompassing curve interpolation, sliding-window SD, and thresholding. The strategy revealed that it is likely to detect pauses of duration over 15 *seconds* in a walk using this approach. However, the strategy may not be suitable for detecting the pauses of two pedestrians simultaneously using this approach since the presence of multiple BLE advertisements may result in packet collisions. To test this hypothesis, in this experiment, two volunteer pedestrians were instructed to walk simultaneously on the pathway 3 *metres* away from the Observer, starting from *start* point and walking towards the *end* point. Pauses are tested at three key points, *approach*, *centre* or *depart*. At each of these locations, three configurations were tested – Broadcasters held in LoS of the Observer by both volunteers, Broadcasters held in nLoS of the Observer by both volunteers and one Broadcaster held in LoS and the other in nLoS of the Observer. GPS measurements were acquired by one of the volunteers through an Android application called GPSLogger.

All the measurements for this experiment were taken on April 9, 2024 between 13:29 and 14:33 hours Irish time with the support from two volunteer pedestrians. The weather information at 13:00 and 14:00 hours on the day of the experiment is following:

**At 13:00 hours on April 9, 2024**

- **Precipitation (Rain):** 0.0 mm
- **Air Temperature:** 11.8 °C
- **Wet Bulb Temperature:** 7.5 °C
- **Dew Point Temperature:** 1.8 °C
- **Vapour Pressure:** 7 hPa
- **Relative Humidity:** 50 %
- **Mean Sea Level Pressure:** 1012.2 hPa

**At 14:00 hours on April 9, 2024**

- **Precipitation (Rain):** 0.0 mm
- **Air Temperature:** 12.6 °C
- **Wet Bulb Temperature:** 7.9 °C
- **Dew Point Temperature:** 1.7 °C
- **Vapour Pressure:** 6.9 hPa
- **Relative Humidity:** 47 %
- **Mean Sea Level Pressure:** 1013 hPa

The collected RSSI values were cycled through the same curve interpolation and sliding-window SD techniques as in the pause detection experiment but, for advertisements for both the Broadcasters separately. The threshold for the SD was chosen to be lower for at least 5 *seconds*. Since the pause duration here is 20 *seconds*, and the advertisement rate is 1.28 *seconds*, the number of advertisements that can be intercepted during the pause period of 20 *seconds* is approximately 15. And, to account for packet collision and packet losses, the thresholding of 20 *seconds*, for just as long as the pause duration, was not viable, as also discussed previously in the Section 2.2.1.

The geolocations acquired from the GPSLogger application were plotted using geoplot and the elapsed time from the start of the walk were posted next to each marker on the geoplot. On the subplot, RSSI was graphed against elapsed time. This allows for easy visual inspection of the RSSI against the ground truth location of the pedestrians. The entire process was applied to each of the 27 individual runs. Here in this dissertation however, only one representative round for each unique case is presented. Figures 2.69, 2.70, and 2.71 represent the charts for the measurements carried out where pedestrians stopped at *approach* location when both Broadcasters were in LoS orientation, where one Broadcaster was in nLoS and the other in LoS, and where both Broadcasters were nLoS of the Observer respectively. The red and blue line-marker combination is used to differentiate the data captured from the two Broadcasters. The phase corresponding to the actual pause in the walk is demarcated by two vertical black lines, whereas, the pause detection through the multi-fold analysis is presented in the red and blue regions on the chart. The overlap of the two regions is magenta in colour.

In Figures 2.69, 2.70, and 2.71, a pause is detected successfully only the LoS-LoS orientation of the two Broadcasters. However, even in the case of successful detection, the pause region exceeded the boundary demarcated by the black lines.

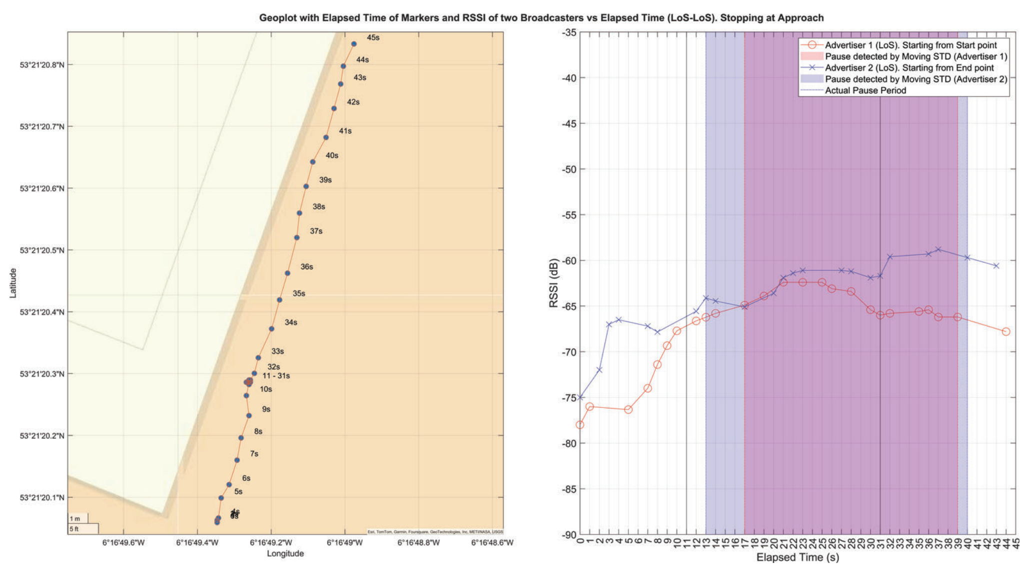


FIGURE 2.69: Geolocation and RSSI vs Elapsed Time Plot when Pedestrians Paused at *Approach* Point, Both Broadcasters in LoS

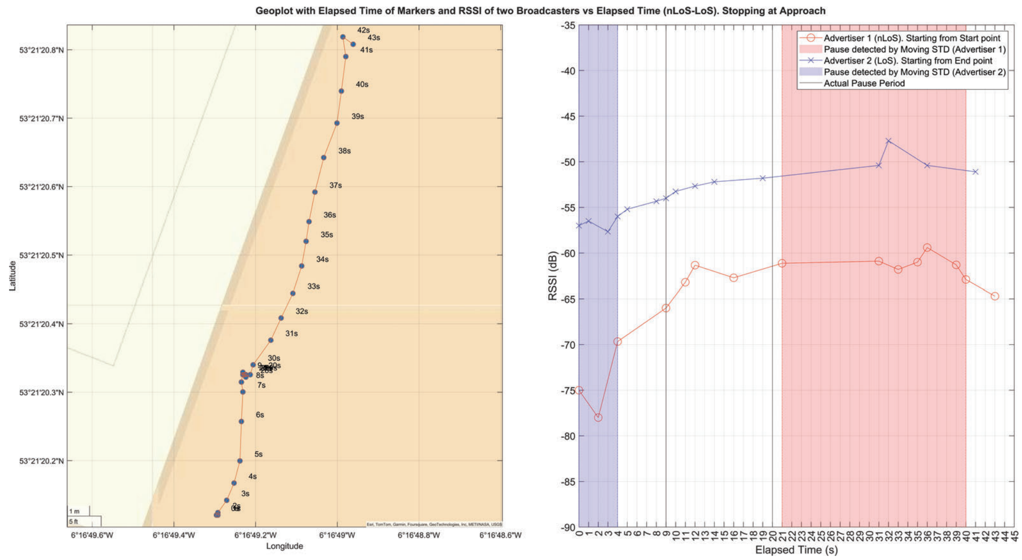


FIGURE 2.70: Geolocation and RSSI vs Elapsed Time Plot when Pedestrians Paused at *Approach* Point, One Pedestrian Carrying Broadcasters in LoS and Other in nLoS

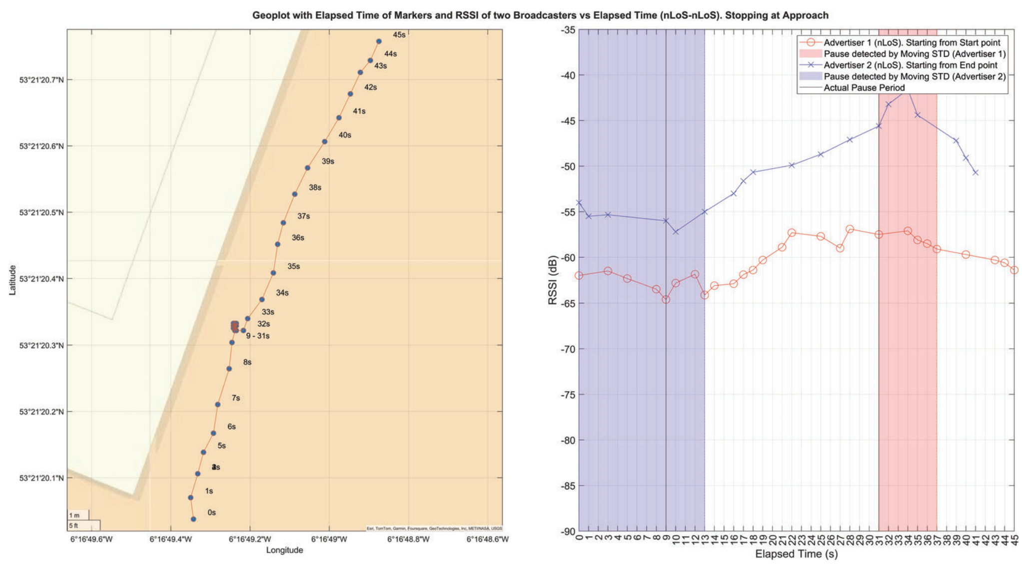


FIGURE 2.71: Geolocation and RSSI vs Elapsed Time Plot when Pedestrians Paused at *Approach* Point, Both Broadcasters in nLoS

Similarly, Figures 2.72, 2.73, and 2.74 represents pausing at the *centre* key point on the pathway in LoS-LoS, LoS-nLoS, and nLoS-nLoS orientations respectively. In this case, in the LoS-LoS orientation, a pause was detected for one advertiser, whereas, in the other two, pause was detected for both the Broadcasters but overshooting the actual pause period.

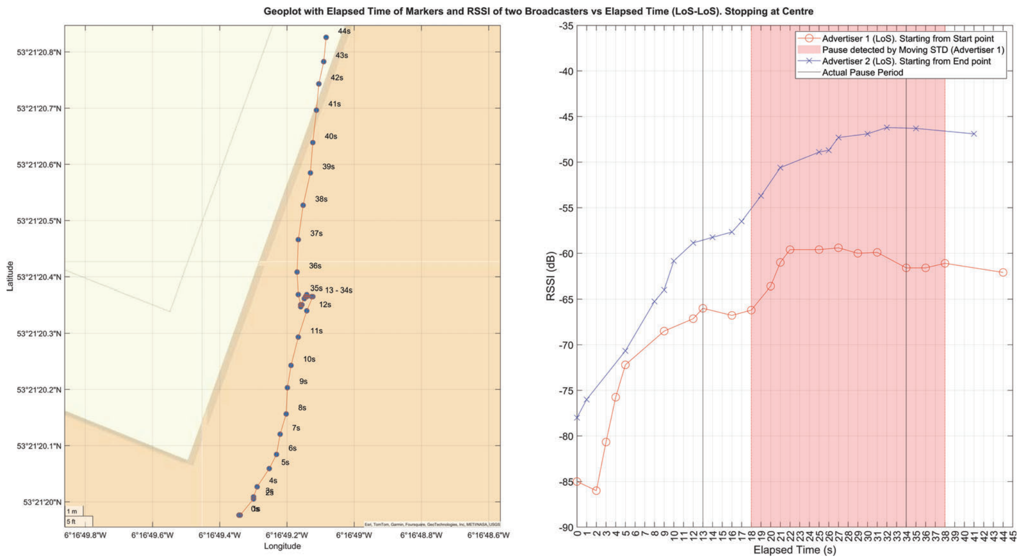


FIGURE 2.72: Geolocation and RSSI vs Elapsed Time Plot when Pedestrians Paused at *Centre* Point, Both Broadcasters in LoS

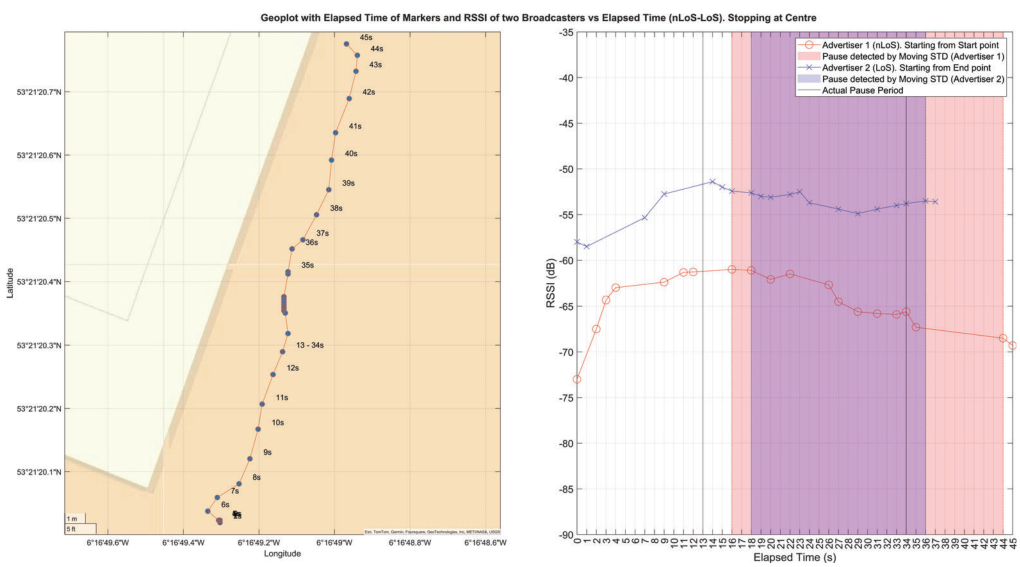


FIGURE 2.73: Geolocation and RSSI vs Elapsed Time Plot when Pedestrians Paused at *Centre* Point, One Pedestrian Carrying Broadcasters in LoS and Other in nLoS

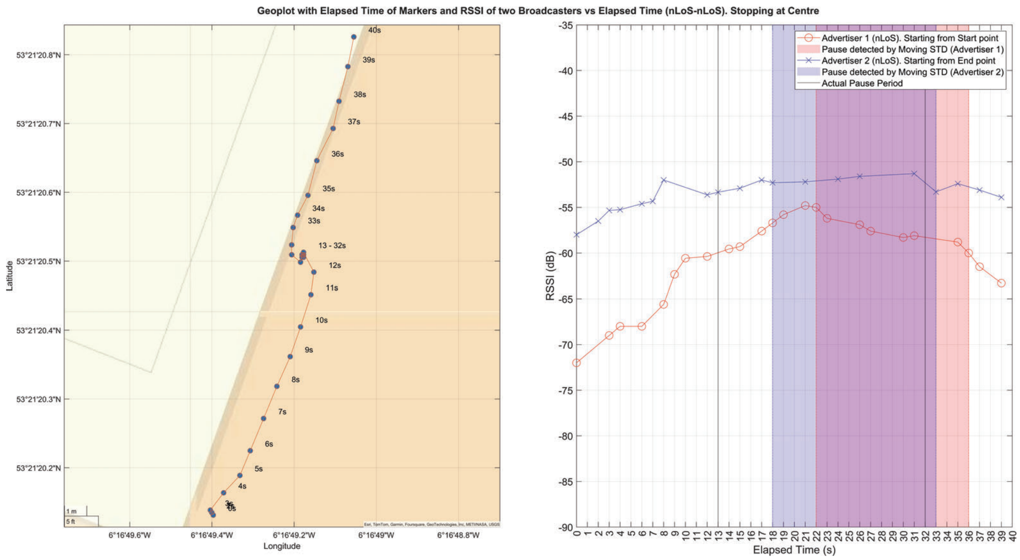


FIGURE 2.74: Geolocation and RSSI vs Elapsed Time Plot when Pedestrians Paused at *Centre* Point, Both Broadcasters in nLoS

Finally, for pause at the *depart* location, a pause was detected for both the Broadcasters in all of the orientations, as seen in Figures 2.75, 2.76, and 2.77. However, the pause period spilled over the actual pauses demarcated even in this case.

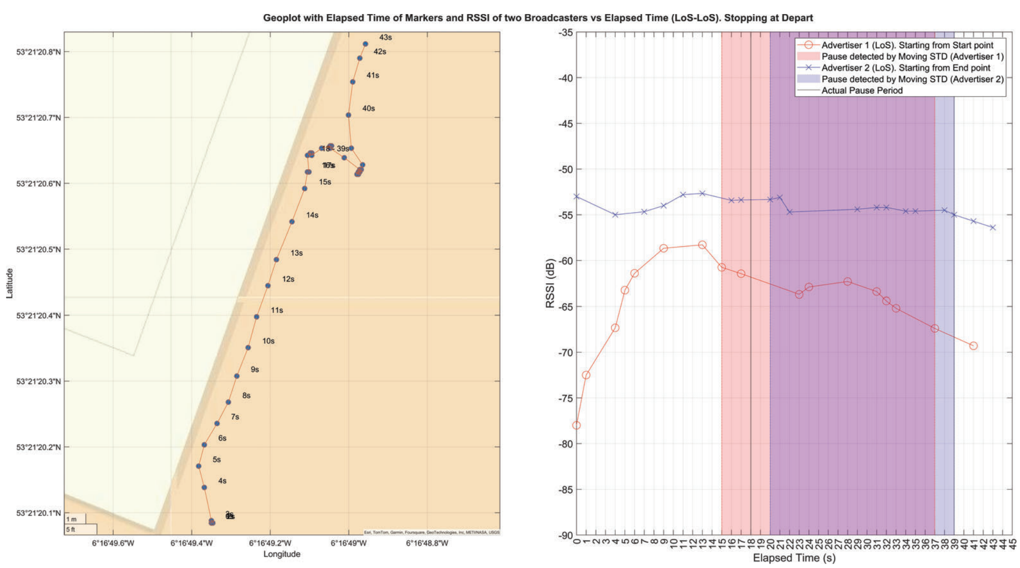


FIGURE 2.75: Geolocation and RSSI vs Elapsed Time Plot when Pedestrians Paused at *Depart* Point, Both Broadcasters in LoS

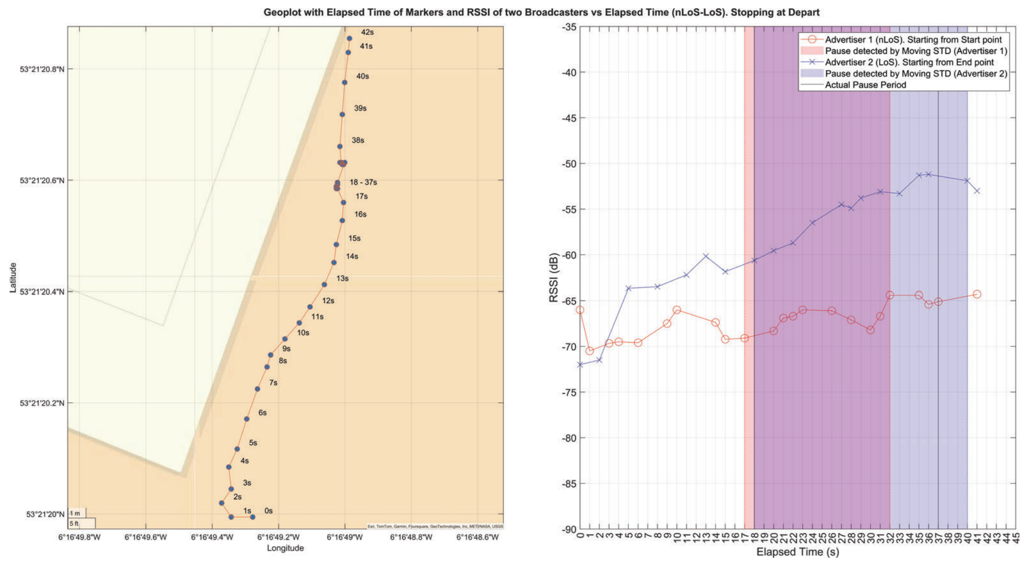


FIGURE 2.76: Geolocation and RSSI vs Elapsed Time Plot when Pedestrians Paused at *Depart* Point, One Pedestrian Carrying Broadcasters in LoS and Other in nLoS

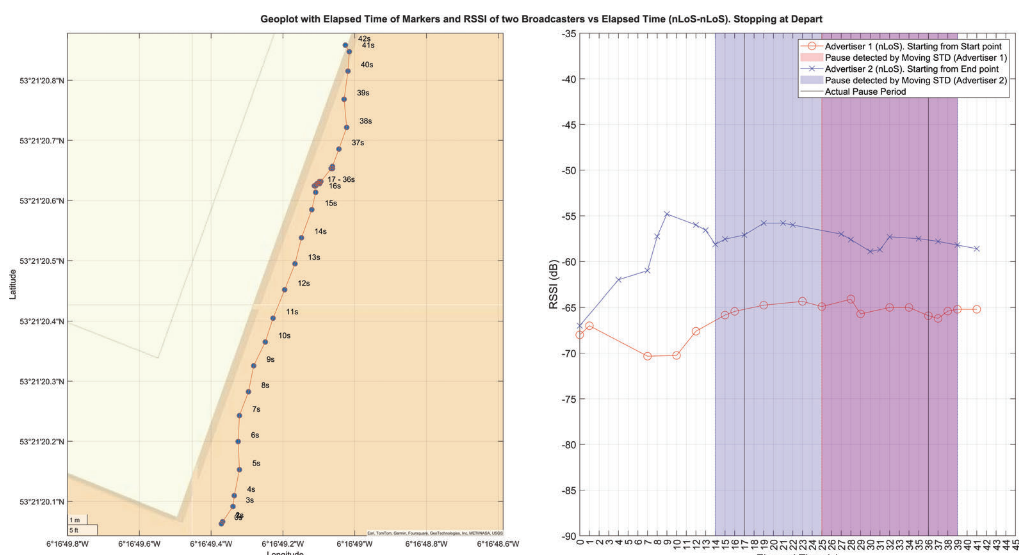


FIGURE 2.77: Geolocation and RSSI vs Elapsed Time Plot when Pedestrians Paused at *Depart* Point, Both Broadcasters in nLoS

From the results, it is clear that the approach identified in the previous experiment 2.2.1, applies to most of the cases when multiple Broadcasters are used simultaneously. However, the output is not accurate enough to pinpoint the exact location of those pauses. Therefore, only a ballpark estimation of the location of the pauses can be estimated. There are many instances in the select cases presented above where the two pause patches overlap. This provides a likelihood of the interaction between the two pedestrians, or, with some element in the environment.

One possible reason for the extension of the detected pause regions could be the clashing advertisements in the same region. While this is not investigated in this PhD, such an investigation to understand the effects of multiple Broadcasters in the same region on the capabilities of the Observer and resulting RSSI will be useful in future work.

Moreover, even when the pause zones are detected, there is insufficient information to treat them as concrete evidence of interaction between the two pedestrians. This is because even when the pauses are identified for the same orientation of Broadcasters, say LoS-LoS, the values of respective RSSI in the detected pause zones are not closely related. For instance, in Figure 2.12, the two detected pause zones overlap, however, the RSSI of Broadcaster 1 in the pause zone is in the range of -67 $dB$ to -62 $dB$, whereas in the same zone, Broadcaster 2 has RSSI close to -55 $dB$. So, if there are no GPS data, it is difficult to predict that both pedestrians stopped at the same location, and their pauses at different locations on the same pathway at the same time could be a mere coincidence. This difference in the RSSI between the two Broadcaster is very likely because the two pedestrians are side-by-side, meaning that the advertisements from the Broadcaster held by the pedestrian on the farther side from the Observer have to travel through some form of partial occlusion caused by the other pedestrian. This is worse when the pedestrian at the farther side is holding the Broadcaster in nLoS, since now, the advertisements from that Broadcaster will interact with the bodies of the two pedestrians while traversing the path to the Observer. This is presented in Figure 2.78.

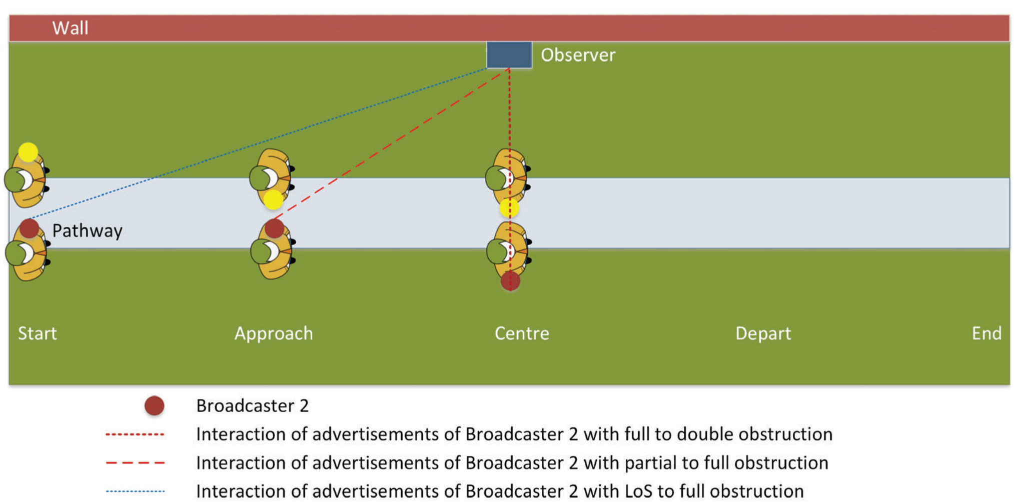


FIGURE 2.78: Obstruction Faced by Advertisement Signals from Broadcaster 2

**Section Summary**

Following on from the previous experiment to detect pauses in the movement of a single pedestrian, Section 2.2.1 of this chapter, an extension to identify pauses in the movement of two pedestrians is carried out in this experiment. With the outcome of the previous experiment, only the likelihood of an interaction is inferred. However, if pauses can be identified in two or more Broadcasters simultaneously, there is an increased likelihood of asserting the interaction between pedestrians.

The collected RSSI are subjected to the same treatment as in the case of the previous experiment. This involved using the curve fitting, sliding-window SD, and thresholding. Since the investigation was already performed to identify the optimal polynomial, for this experimental setup, and the size of the sliding window previously, those parameters are not re-evaluated again. The results reveal the consistency of the approach as it can detect pauses for both the Broadcasters in most of the cases tested. It is however not possible to pinpoint the location of the pauses as the detected pause locations have extended beyond the actual pause zones due to the range of RSSI values differing from one another significantly in the pause regions. It is reasonable to believe that the presence of two Broadcasters in the same region also increases the chances of packet collision, subsequently leading to packet loss. However, this is not part of the investigation in this PhD.

### 2.2.3 Asserting the Direction of Travel

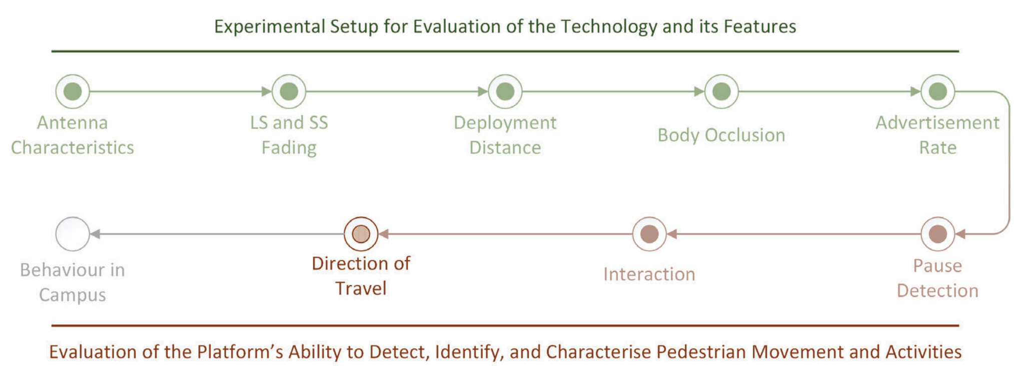


The learning from 2.1.1 was employed in this experiment to identify the direction of travel of the volunteer pedestrian. Through that experiment, it was found that the antenna on the Observer used in this study was more sensitive towards signals emerging from the *approach* region or the 45° region with respect to the horizontal plane of the Observer. Therefore, if the entire journey, or in other words, all the RSS values collected throughout the journey of the pedestrian are divided into two parts, the stronger reception of the signals, as represented by the collected RSSI, should be obtained towards the side of the journey that happened around the 45° region along the plane of the Observer antenna.

Data for this experiment was collected on May 25, 2023 between 11:35 and 12:27 hours Irish time with the support from a single volunteer pedestrian. The weather information at 11:00 and 12:00 hours on the day of the experiment is following:

**At 11:00 hours on May 25, 2023**

- **Precipitation (Rain):** 0.0 mm
- **Air Temperature:** 17.9 °C
- **Wet Bulb Temperature:** 11.7 °C
- **Dew Point Temperature:** 5.0 °C
- **Vapour Pressure:** 8.7 hPa
- **Relative Humidity:** 42 %
- **Mean Sea Level Pressure:** 1033.2 hPa

**At 12:00 hours on May 25, 2023**

- **Precipitation (Rain):** 0.0 mm
- **Air Temperature:** 18.8 °C
- **Wet Bulb Temperature:** 11.9 °C
- **Dew Point Temperature:** 4.4 °C
- **Vapour Pressure:** 8.4 hPa
- **Relative Humidity:** 38 %
- **Mean Sea Level Pressure:** 1032.9 hPa

The experiment was divided into two cases, first, where the Observer and Broadcaster were in LoS, and second, where the two devices were in nLoS. Each scenario was repeated three times and on two pathways, situated 3 *metres* and 5 *metres* away from the deployed Observer. Also, two scenarios were devised, first where the pedestrian started walking from the *start* point to the *end* point and second, where the journey was started from the *end* point to the *start* point. Every case and scenario was repeated 3 times. The *Blue Dot* app was used to collect the actual location of the volunteer pedestrian as ground truth. The location obtained from *Blue Dot* was used to divide the collected RSS values into two segments.

The collected RSS values for each half of the journeys were averaged and compared to identify whether the reception of the signals was stronger on the side of the path where the antenna of the Observer was more sensitive or not. This result is summarised in Table 2.15.

Looking at the pedestrian walks from the *start* point to the *end* point in the case where the path is 3 *metres* away from the Observer, it was observed that there was only one journey, in both LoS and nLoS scenarios combined, that had a higher mean RSS value in the region between the *centre* point and the *end* point. Further, averaging all of the mean RSS values for both scenarios combined, categorised by the region in which the walk took place, journey between the *start* point to the *centre* point were observed to have an average RSS value of -61.85 *dB* and that between the

| Mean RSSI from Start to End region | | | | | | |
|---|---|---|---|---|---|---|
| **Case** | Rep 1 (dB) | | Rep 2 (dB) | | Rep 3 (dB) | |
| | S → C [1] | C → E [2] | S → C | C → E | S → C | C → E |
| **3m LoS** | -57.68 | -64.47 | -61.82 | -67.75 | -63.53 | -59.88 |
| **3m nLoS** | -60.25 | -76.75 | -63.38 | -73.13 | -65.25 | -66.50 |
| **5m LoS** | -59.97 | -64.27 | -65.64 | -64.66 | -59.23 | -65.47 |
| **5m nLoS** | -67.61 | -65.78 | -65.83 | -68.28 | -66.96 | -70.23 |
| **Mean RSSI from End to Start region** | | | | | | |
| **Case** | Rep 1 (dB) | | Rep 2 (dB) | | Rep 3 (dB) | |
| | E → C [3] | C → S [4] | E → C | C → S | E → C | C → S |
| **3m LoS** | -68.93 | -64.16 | -64.19 | -59.58 | -77.77 | -63.88 |
| **3m nLoS** | -75.42 | -69.28 | -71.16 | -67.22 | -74.38 | -62.54 |
| **5m LoS** | -63.33 | -61.60 | -57.29 | -67.17 | -65.81 | -63.41 |
| **5m nLoS** | -80.53 | -70.40 | -66.47 | -67.38 | -72.29 | -68.59 |

[1] Start → Centre.
[2] Centre → Start.
[3] End → Centre.
[4] Centre → Start.

TABLE 2.15: Mean RSS Value Between the Two Parts of the Journey for Each Deployment Distance for Both LoS and nLoS Cases

*centre* point to the end point had an average RSS value of -67.64 *dB*. This was consistent with expectations based on the results obtained from the experiment conducted in 2.1.1 presented in this chapter.

Similarly, at a deployment distance of 5 *metres*, two occurrences of higher mean RSS values in the region between the *centre* and *end* point out of six total journeys were observed. The average of the mean RSS values between the start to the centre region was -64.20 *dB*, whereas, the equivalent for the centre-to-end part of the journey was -66.45 *dB*. Again, this was consistent with the results obtained at the 3-*metre* deployment distance.

For journeys that started at the *end* point and finished at the *start* point, the outcome was similar. At a deployment distance of 3 *metres*, there was no instance out of the six repetitions combined across LoS and nLoS cases where the mean RSS value during the journey between the *end* point and the *centre* point was higher than that of the journey between the *centre* point and *start* point. The average of mean RSSI for the former was -70.98 *dB*, whereas that for the latter was -64.44 *dB*. At a distance of 5 *metres*, there were two occasions out of six where the mean RSS values for a journey between the *end* to the *centre* point was greater than that at the *centre* to the *start* point. The average of those means had a marginal difference but nevertheless, was in favour of the journey between the *centre* and the *start* region with the value of -66.42 *dB* against -67.62 *dB*.

Out of the combined 24 cases, a higher mean RSS value was found between the centre and end region 5 times, that is for 20.83% of all the cases. This implies that there was a high likelihood, 79.17% to be exact, of identifying the direction of travel of the pedestrian through simple mean calculation of the collected RSS values. Looking at the charts, however, the double hump pattern discussed in the earlier experiment, in Section 2.1.1 in this chapter, was a rarity outside of the anechoic chamber. This could be due to the strong LoS component found at the *approach* and *centre* key points and the effect of shadowing observed at *depart* key point, as was identified in the outcome of experiment presented in Figure 2.5 and Table 2.3 of Section 2.1.2 in this chapter. Figures 2.79, 2.80, 2.81, and 2.82 depict the chart of RSSI against elapsed time, with pseudo-names of the location on the path mentioned in the x-axis obtained through the Blue Dot app, for the 3 *metres* deployment distance LoS, 3 *metres* deployment distance nLoS, 5 *metres* deployments distance LoS and 5 *metres* deployment distance nLoS. On the second y-axis, the charts also depict the number of advertisements obtained per second during the walk between each subsequent location on the path. It can be seen on those figures that the advertisement rate at the Observer dropped in the case of nLoS. This result was also consistent with the results obtained from the experiment to test the effect of body occlusion, described in Section 2.1.4 in this chapter. The averaged duration, samples, and sample count for each distance and case are presented in Table 2.16

| **Locations** | **3 *metres* LoS** | | |
|---|---|---|---|
| | Duration (s) | Samples | Samples per second |
| **Start → Approach** | 5.40 | 5.25 | 0.97 |
| **Approach → Centre** | 5.06 | 4.16 | 0.82 |
| **Centre → Depart** | 5.52 | 5.16 | 0.93 |
| **Depart → End** | 5.58 | 5.08 | 0.91 |
| | **3 *metres* nLoS** | | |
| **Start → Approach** | 5.06 | 3.92 | 0.77 |
| **Approach → Centre** | 4.88 | 3.92 | 0.80 |
| **Centre → Depart** | 5.06 | 4.50 | 0.89 |
| **Depart → End** | 4.85 | 3.50 | 0.72 |
| | **5 *metres* LoS** | | |
| **Start → Approach** | 5.01 | 4.58 | 0.91 |
| **Approach → Centre** | 4.95 | 4.67 | 0.94 |
| **Centre → Depart** | 5.14 | 5.08 | 0.99 |
| **Depart → End** | 4.78 | 3.3 | 0.70 |
| | **5 *metres* nLoS** | | |
| **Start → Approach** | 5.64 | 4.25 | 0.75 |
| **Approach → Centre** | 5.18 | 4.5 | 0.87 |
| **Centre → Depart** | 5.57 | 4.75 | 0.85 |
| **Depart → End** | 5.34 | 3.83 | 0.72 |

TABLE 2.16: Mean Duration and Samples at Each Deployment Distance for Both LoS and nLoS Cases

**Section Summary**

Detection of direction is a useful measure to understand the usage pattern of a pathway and to characterise the usage requirements of the pedestrians from the pathway. It is an easier task to solve with BLE by using multiple Observers and placing them strategically such that the strength of signals in one Observer is faded when the pedestrian is close to the other Observer and vice versa. However, achieving this with a single Observer is a challenge. While modern versions of BLE, version 5.1 and onwards inherently provide

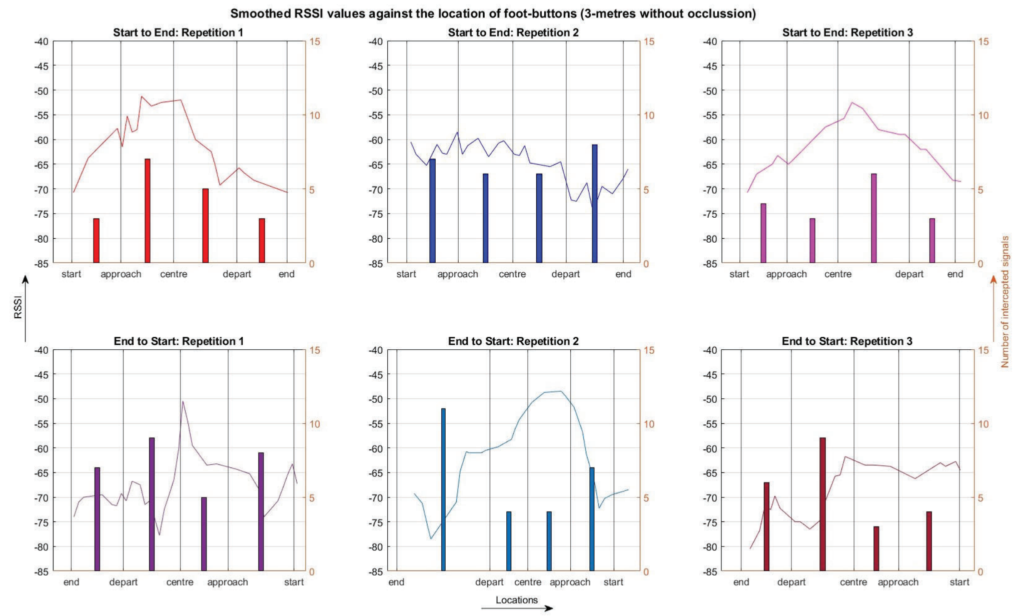


FIGURE 2.79: RSSI values of a Broadcaster in LoS of Observer when the Pedestrian is Walking on a Pathway 3-*metres* Away, LoS

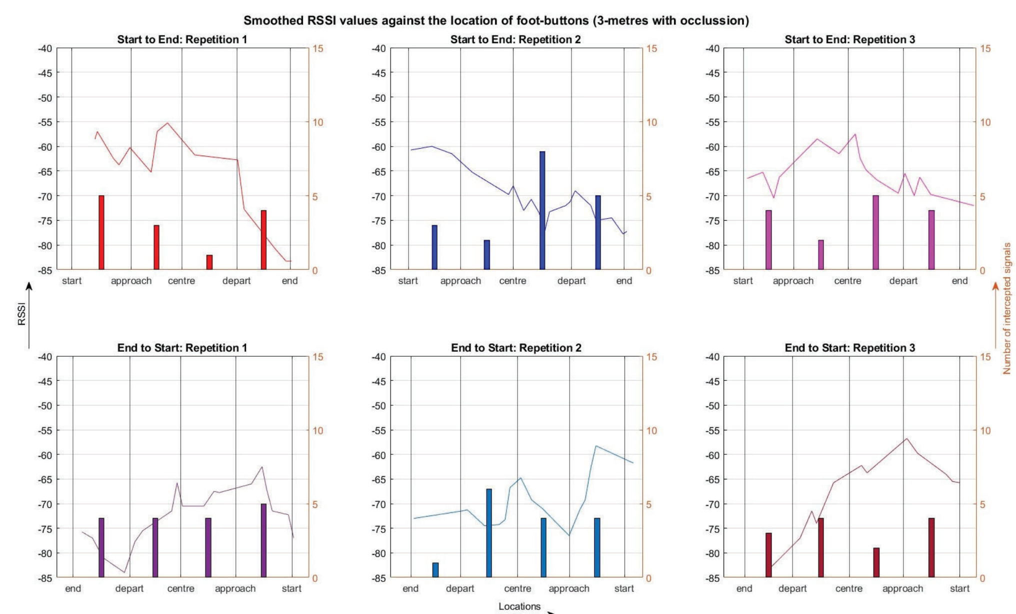


FIGURE 2.80: RSSI values of a Broadcaster is in nLoS of Observer when the Pedestrian is Walking on a Pathway 3-*metres* Away

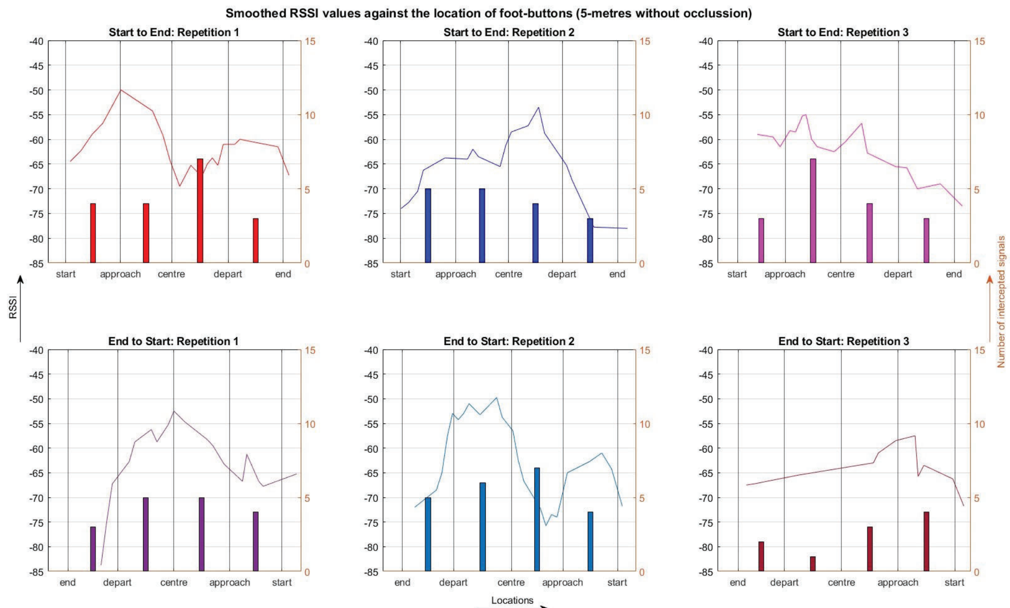


FIGURE 2.81: RSSI values of a Broadcaster in LoS of Observer when the Pedestrian is Walking on a Pathway 5-*metres* Away

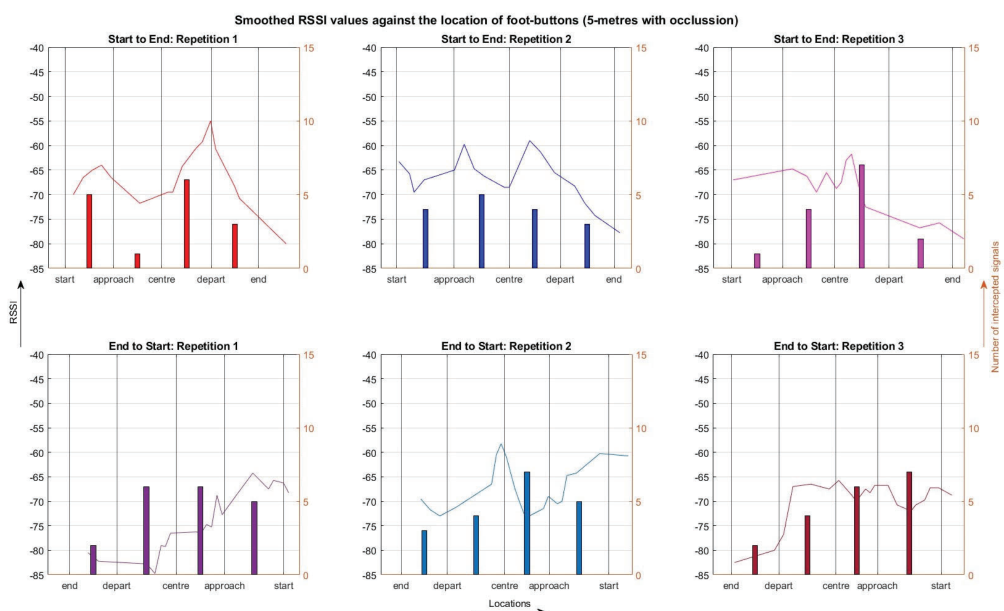


FIGURE 2.82: RSSI values of a Broadcaster is in nLoS of Observer when the Pedestrian is Walking on a Pathway 5-*metres* Away

this capability by detecting the angle of arrival of signals, previous versions of BLE lack this functionality. Although, BLE 5.1 was released in January 2019 (Bluetooth SIG, 2019), the most recent version, version 5, of one of the market leading SBC, RPi which was released in 2023, comes with BLE v5.0. Throughout the course of this experiment, from conceptualised to publication, the most recent RPi device was version 4B, which used BLE version 4.0. I conceptualised this research experiment based on the results of the antenna characteristics experiment presented in section 2.1.1. The results of those experiments revealed the sensitivity of the antenna on the Observer towards the signals arising between 0° and 90° region, and therefore, this characteristic of the antenna favoured signals from one direction over the other.

The pattern in the RSS values here is not apparent when the plots of those values against time are observed and the results look inconclusive. However, some basic statistics unearth nuances that are useful for forming assertions. By dividing each journey into phases, travelling to and from the *start* and *centre*, and to and from the *centre* and *end*, we are able to see that the mean of the SMA-filtered RSS values is higher for travelling in either direction between the *start* and *centre* region. If we know the orientation of the Observer and the topology of the surrounding environment, through the temporal location of the onset of that local peak, we can identify the direction of travel. In other words, a sharp climb to the local peak RSS value is followed by a long tail with the possibility of a second lesser peak (double hump) when the direction of travel is from start to end. And, a slow climb with a lesser peak followed by a local peak and a sharp decline when the travel direction is reversed. Moreover, as learnt from the results of the previous experiments 2.1.4, the sample rate identified in Table 2.16 is also indicative of interference between the Observer and the Broadcaster as the number of samples per second in the nLoS case is consistently lesser compared to the LoScase. While the likelihood of asserting the direction of travel of a pedestrian in a linear pathway using a single Observer by exploiting the characteristics of its antenna is proven through the results, the uncertainties in the environment affect the performance and hence the confidence of the assertions. The chosen pathway here is infrequently used and is devoid of large physical objects. If these factors are present, the likelihood of inference could result in less reliable inferences.

The results of this experiment are presented in the paper titled, "Indication of pedestrians travel direction through Bluetooth Low Energy signals perceived by a single Observer device" (Parmar, Kelly, and Berry, 2023b).

### 2.2.4 Analysing the Behaviour of Pedestrians in a University Campus for an Extended Period

This experiment was a long-term study of pedestrian behaviour in a university campus in which a total of 17 Broadcasters (mix of indoor RPi-based and outdoor ESP32-based) were employed. Measurements were obtained from 28 active volunteers, totalling 272 pedestrian journeys undertaken, and aggregated. The aggregated data was then analysed. Table 2.17 presents counts of the BLE events or advertisements

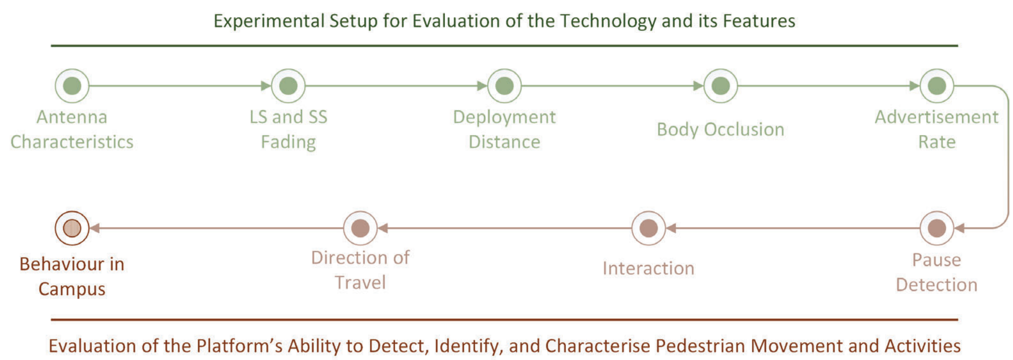


that are observed for 24 days of the experiment at each location by each volunteer pedestrian. The presented data appears rudimentary, lacking any statistical analysis, however, through this data, utilisation of the regions of the observed part of the campus was derived. For instance, the *Pedestrian Pathway* reported the highest number of detected advertisements, meaning that it was widely used by volunteer pedestrians. It was important to note that just under half of these advertisements on the *Pedestrian Pathway* result from the BLE Broadcaster carried by one particular volunteer. Even if this was consider as an outlier, a median of the count of advertisements, that can suppress the effect of outliers (Wilcox, 2021), suggests that the *Pedestrian Walkway* was still the most frequently visited place on the campus by the participating volunteers. Similarly, the data in the table indicated that places like *Constitution Hill*, *Beresford*, *Broadstone Luas*, *Rathdown Store*, and *Kirwan Street* were less visited by the volunteers.

Moreover, the captured data also provided information at a finer level of granularity, for instance, Figure 2.83 shows the aggregated RSSI record of one of the individual participating pedestrians for what appears to be a 30-*minute* morning walk. The figure shows that the detected advertisements for this volunteer lead to a sequence of RSS values that reflect the journey of the said pedestrian. Bearing in mind that RSSI between -70 *dB*s and -80 *dB*s can be associated with a passing pedestrian at a distance of 10 to 20 *m* from an Observer (Alanbouri et al., 2019), it was possible to infer the approximate trajectory of the pedestrian from the locations of the Observers.

Figure 2.83 depicts the inferred path of that pedestrian as an example. The numbers 1 through 6 on the figure are further represented on a map in Figure 2.84. From a comparison of the RSSI record and the campus map, the volunteer entered the campus through one of the main campus gates, and performed a circuit of one part of the campus over a period of 30 *minutes* before exiting through the same gate. Another impactful estimation identified about a pedestrian's behaviour from this data was their pace of travel. Considering Figure 2.83, approximate time of proximity of the pedestrian to the Observers was identified. The approximate times when the pedestrian was at each of those locations were obtained from timestamps and were correlated against the distance between these locations. The distances between these locations were obtained using open mapping software. the probable pace of the pedestrian was then assessed with this information. Table 2.18 provides the distances between the locations traversed by the pedestrian, and based on the trajectory

| Volunteer ID | Locations | | | | | | | | | | | | | | | | |
|---|---|---|---|---|---|---|---|---|---|---|---|---|---|---|---|---|---|
| | Constitution Hill | Breseford | Broadstone LUAS | GG LUAS | Clocktower Meeting | Clocktower Office | Rathdown Office | Rathdown Store | Northhouse Art | Northhouse Annex | Blend Cafe | Fingal Place | Pedestrian Pathway | Kirwan St | GG by church | Parkhouse | HSE gate |
| 2 | 0 | 44 | 0 | 158 | 30 | 259 | 37 | 0 | 145 | 69 | 211 | 0 | 13 | 0 | 264 | 154 | 798 |
| 3 | 0 | 4 | 0 | 0 | 2 | 8 | 9 | 0 | 103 | 22 | 179 | 0 | 19 | 0 | 55 | 105 | 346 |
| 4 | 0 | 0 | 0 | 0 | 0 | 2 | 1 | 0 | 0 | 0 | 0 | 0 | 0 | 0 | 78 | 0 | 0 |
| 5 | 181 | 3 | 175 | 3 | 19 | 90 | 71 | 0 | 12 | 426 | 0 | 18 | 885 | 6 | 512 | 3 | 0 |
| 6 | 1 | 0 | 0 | 102 | 138 | 2009 | 781 | 54 | 846 | 2705 | 61 | 1497 | 2646 | 0 | 4909 | 121 | 77 |
| 7 | 1 | 9 | 0 | 84 | 211 | 1980 | 1360 | 102 | 746 | 3486 | 450 | 502 | 2590 | 42 | 9352 | 84 | 494 |
| 8 | 18 | 0 | 14 | 0 | 0 | 1 | 0 | 0 | 952 | 866 | 270 | 133 | 1513 | 0 | 500 | 1004 | 689 |
| 9 | 0 | 0 | 0 | 0 | 0 | 0 | 0 | 0 | 0 | 0 | 0 | 0 | 147 | 0 | 0 | 0 | 0 |
| 10 | 0 | 7 | 0 | 54 | 31 | 142 | 132 | 0 | 13 | 630 | 0 | 16 | 684 | 0 | 1243 | 0 | 0 |
| 12 | 0 | 0 | 0 | 0 | 0 | 0 | 4 | 0 | 0 | 0 | 0 | 0 | 0 | 0 | 0 | 0 | 0 |
| 13 | 81 | 0 | 112 | 24 | 41 | 344 | 30 | 37 | 0 | 19 | 0 | 0 | 2 | 0 | 8 | 0 | 9 |
| 14 | 0 | 0 | 0 | 114 | 53 | 829 | 34 | 75 | 135 | 345 | 451 | 4 | 41 | 0 | 77 | 186 | 244 |
| 15 | 1 | 0 | 0 | 13 | 0 | 23 | 16 | 0 | 4 | 80 | 0 | 11 | 132 | 53 | 127 | 2 | 0 |
| 16 | 0 | 0 | 0 | 52 | 60 | 339 | 74 | 38 | 58 | 558 | 0 | 41 | 888 | 1 | 767 | 17 | 15 |
| 17 | 56 | 0 | 2 | 47 | 18 | 293 | 13 | 7 | 53 | 292 | 77 | 35 | 251 | 0 | 167 | 157 | 175 |
| 18 | 0 | 0 | 0 | 12 | 11 | 40 | 19 | 0 | 14 | 523 | 54 | 57 | 335 | 87 | 323 | 0 | 0 |
| 19 | 0 | 1 | 0 | 24 | 4 | 57 | 39 | 0 | 4 | 185 | 0 | 12 | 1762 | 110 | 339 | 0 | 0 |
| 20 | 0 | 2 | 1 | 72 | 30 | 179 | 53 | 24 | 23 | 609 | 0 | 45 | 640 | 0 | 753 | 53 | 34 |
| 21 | 3 | 13 | 0 | 63 | 58 | 340 | 124 | 31 | 255 | 380 | 62 | 32 | 1004 | 9821 | 1401 | 133 | 102 |
| 22 | 0 | 0 | 0 | 826 | 215 | 2004 | 299 | 212 | 909 | 2523 | 0 | 147 | 1486 | 0 | 786 | 36 | 123 |
| 23 | 31 | 0 | 21 | 123 | 118 | 752 | 626 | 0 | 546 | 1721 | 68 | 282 | 14921 | 622 | 1981 | 50 | 29 |
| 24 | 0 | 0 | 0 | 49 | 60 | 313 | 212 | 0 | 159 | 647 | 336 | 102 | 662 | 150 | 508 | 33 | 41 |
| 25 | 3 | 5 | 8 | 442 | 39 | 354 | 94 | 20 | 219 | 490 | 253 | 82 | 1103 | 258 | 1251 | 47 | 98 |
| 26 | 1 | 11 | 0 | 45 | 22 | 332 | 100 | 30 | 57 | 212 | 41 | 44 | 230 | 125 | 461 | 82 | 102 |
| 27 | 0 | 0 | 0 | 11 | 12 | 64 | 33 | 0 | 19 | 221 | 67 | 84 | 336 | 61 | 302 | 0 | 0 |
| 28 | 13 | 0 | 0 | 7 | 7 | 105 | 28 | 0 | 123 | 266 | 206 | 98 | 403 | 63 | 262 | 96 | 88 |
| 29 | 0 | 0 | 0 | 5 | 3 | 31 | 13 | 0 | 15 | 193 | 0 | 0 | 112 | 33 | 126 | 4 | 9 |
| 30 | 9 | 4 | 16 | 24 | 8 | 51 | 13 | 0 | 0 | 0 | 12 | 0 | 2 | 313 | 87 | 0 | 0 |
| **Total** | 399 | 103 | 349 | 2354 | 1190 | 10941 | 4215 | 630 | 5410 | 17468 | 2798 | 3242 | 32807 | 11745 | 26639 | 2367 | 3473 |
| **Median count** | 0 | 0 | 0 | 34.5 | 20.5 | 160.5 | 35.5 | 0 | 55 | 318.5 | 47.5 | 33.5 | 369.5 | 3.5 | 331 | 34.5 | 31.5 |

TABLE 2.17: Number of BLE Events for All Volunteers at Each Location.

which passed through points 1 2 3 4 5 6 2 1, the volunteer travelled 1475 *m* in approximately 30 *minutes*, resulting in a mean walking pace of 0.8 *m* per *second*, indicating brisk walking pace.

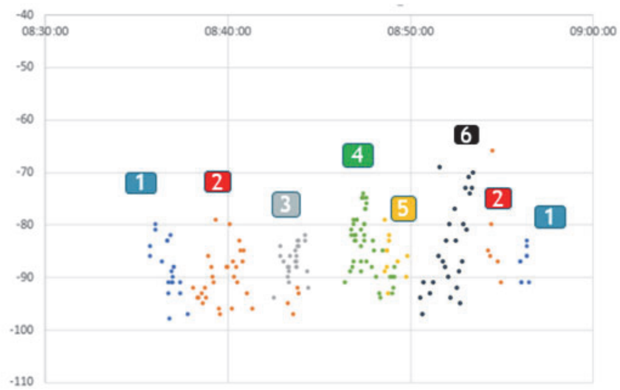


FIGURE 2.83: Scattered RSS of Observed Advertisement by Different Observers from a Single Volunteer Pedestrian Representing a Journey: Example 1.

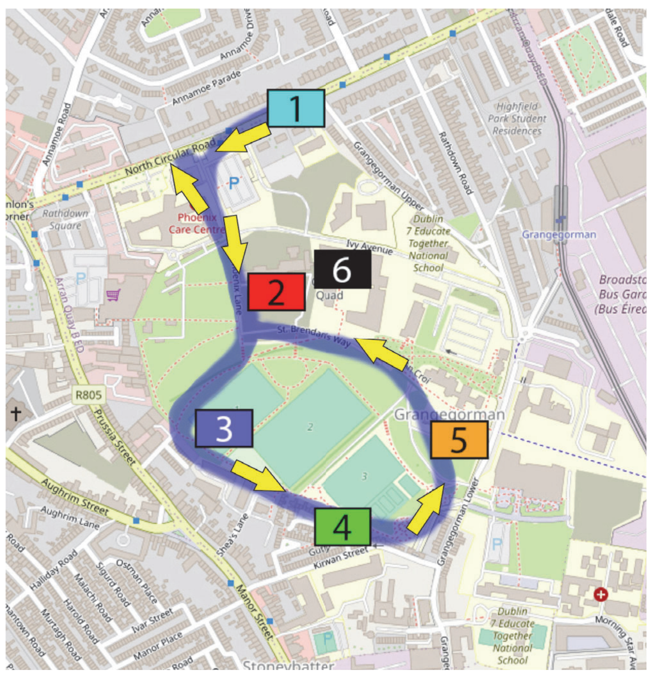


FIGURE 2.84: Journey Estimation of a Selected Pedestrian: Example 1.

This study suggests the usefulness of BLE to understand the behaviour of pedestrians and subsequently, estimate the utilisation of spaces. A mere counting of observed advertisements emanating from beacons carried by volunteer pedestrians over an extended period of time has been seen to be sufficient in identifying aggregated insights of space utilisation. This is favourable from the privacy preservation point of view since the presented method neither requires personal identification nor personal data. Through the RSSI record for an individual volunteer, it is possible to

| *Origin* to *Destination* | Distance |
|---|---|
| Location 1 to Location 2 | 275 m |
| Location 2 to Location 3 | 175 m |
| Location 3 to Location 4 | 150 m |
| Location 4 to Location 5 | 150 m |
| Location 5 to Location 6 | 400 m |
| Location 6 to Location 2 | 50 m |

TABLE 2.18: Distances in Metres Between Locations 1 to 6 from Figure 2.83.

infer details of their journey and estimate the walking pace of the pedestrian. Such information is useful to identify frequently used routes and the type of pedestrian using the route, whether casual or purposeful. A casual or leisurely walker may walk at a slower pace and may even make stops along the journey. These crucial details are, as presented, easy to identify through this approach.

The presented experimental data also poses a challenge. For instance, a higher advertisement count is observed from volunteer number 23 at the Pedestrian Pathway, volunteer 21 at Kirwan St., and volunteer 7 at GG by the church. This presents a likelihood that these volunteers may either reside close to this space or work in the vicinity. Identification of such information limits the privacy preservation aspect of the technology. Therefore, future studies should aim to explore methods to mitigate such concerns.

**Section Summary**

This study is a pilot use of BLE as a holistic pedestrian behaviour monitoring system. Through this study, it is possible to identify the choice of activity, for example, leisurely walking or commuting to work, through the estimation of the pace of the pedestrian. This behaviour corresponds to the strategic level behaviour. The choice of route, and entry and exit points are also identifiable in this experiment, which corresponds to the tactical level behaviour. Finally, the local interaction of the pedestrian is also identifiable through the observation of an extended period of BLE advertisements at a given location. There is a likelihood of further categorisation of the local interaction with the spaces or interactions with other pedestrians if other pedestrians are also participating in the experiment and happen to take a pause at the same time, at the same place, and for the same duration as with another participating pedestrian. However, this is not studied in this experiment. Regardless, this attribute corresponds to the operational-level behaviour. Thus, this study encompasses all the pedestrian behaviour types using BLE. It is noteworthy that no sophisticated algorithm was used in the analysis, which provides this approach with an edge over other monitoring techniques.

The study presented in this section is published in a paper titled, Capturing the Behaviour of Volunteer Pedestrians in a Newly-developed University Campus using a Distributed Array of Bluetooth Low Energy devices (AlAnbouri et al., 2023), where my contribution as a second author was the identification of part of the contributions, the analysis of the portion of the data reported here, and significant input on co-authoring the paper.

# Bibliography

*@abandonware/noble - npm* (n.d.). URL: https://www.npmjs.com/package/@abandonware/noble.

Abedi, Naeim, A. Bhaskar, and E. Chung (2013). "Bluetooth and Wi-Fi MAC Address Based Crowd Data Collection and Monitoring: Benefits, Challenges and Enhancement." In: *Australasian Transport Research Forum*.

Acar, Abbas et al. (2018). "A Survey on Homomorphic Encryption Schemes: Theory and Implementation." In: *ACM Comput. Surv.* 51.4. ISSN: 0360-0300. DOI: 10.1145/3214303. URL: https://doi.org/10.1145/3214303.

Ajzen, Icek (1985). "From Intentions to Actions: A Theory of Planned Behavior." In: *Action Control*, pp. 11–39. DOI: 10.1007/978-3-642-69746-3_2. URL: https://link.springer.com/chapter/10.1007/978-3-642-69746-3_2.

Al-Azzawi, Marwan and Robert Raeside (Sept. 2007). "Modeling Pedestrian Walking Speeds on Sidewalks." In: *Journal of Urban Planning and Development* 133 (3), pp. 211–219. ISSN: 0733-9488. DOI: 10.1061/(ASCE)0733-9488(2007)133:3(211). URL: https://ascelibrary.org/doi/abs/10.1061/%28ASCE%290733-9488%282007%29133%3A3%28211%29https://ascelibrary.org/doi/10.1061/%28ASCE%290733-9488%282007%29133%3A3%28211%29.

Alanbouri, Ahlam et al. (2019). "Using Bluetooth Low Energy devices to monitor visitor activity in remote amenity spaces." In: *Irish Transport Research Network*.

AlAnbouri, Ahlam et al. (Oct. 2023). "Capturing the Behaviour of Volunteer Pedestrians in a Newly-Developed University Campus Using a Distributed Array of Bluetooth Low Energy Devices." In: pp. 1–7. DOI: 10.1109/ISC257844.2023.10293279.

*Ansmann Powerbank* (n.d.). URL: https://uk.rs-online.com/web/p/power-banks/1350999.

BeagleBoard (2023). *BeagleBoneő Black - BeagleBoard*. URL: https://www.beagleboard.org/boards/beaglebone-black.

Bier, Eric et al. (Nov. 2009). "The rules of redaction: Identify, protect, review (and Repeat)." In: *IEEE Security and Privacy* 7 (6), pp. 46–53. ISSN: 15407993. DOI: 10.1109/MSP.2009.183.

Blanke, Ulf et al. (2014). "Capturing crowd dynamics at large scale events using participatory GPS-localization." In: *IEEE ISSNIP 2014 - 2014 IEEE 9th International Conference on Intelligent Sensors, Sensor Networks and Information Processing, Conference Proceedings*. DOI: 10.1109/ISSNIP.2014.6827652.

*Blue Dot - Apps on Google Play* (n.d.). URL: https://play.google.com/store/apps/details?id=com.stuffaboutcode.bluedot.

Bluetooth SIG (Jan. 2019). *Bluetooth Core Specification Version 5.1*. Available: https://www.bluetooth.com/specifications/bluetooth-core-specification/.

*BlueZ* (n.d.). URL: http://www.bluez.org/.

Boltes, Maik et al. (2010). "Automatic Extraction of Pedestrian Trajectories from Video Recordings." In: *Pedestrian and Evacuation Dynamics 2008*, pp. 43–54. DOI: 10.1007/978-3-642-04504-2_3. URL: https://link.springer.com/chapter/10.1007/978-3-642-04504-2_3.

Bonne, Bram et al. (2013). "WiFiPi: Involuntary tracking of visitors at mass events." In: *2013 IEEE 14th International Symposium on a World of Wireless, Mobile and Multimedia Networks, WoWMoM 2013*. DOI: 10.1109/WOWMOM.2013.6583443.

Cai, Bolun, Xiangmin Xu, and Dacheng Tao (2016). "Real-Time Video Dehazing Based on Spatio-Temporal MRF." In: *Pacific Rim Conference on Multimedia*. Springer, pp. 315–325.

*Configuration - Raspberry Pi Documentation* (n.d.). URL: https://www.raspberrypi.com/documentation/computers/configuration.html.

Daamen, Winnie and Serge P. Hoogendoorn (Jan. 2003). "Experimental Research of Pedestrian Walking Behavior." In: *https://doi.org/10.3141/1828-03* (1828), pp. 20–30. ISSN: 03611981. DOI: 10.3141/1828-03. URL: https://journals.sagepub.com/doi/10.3141/1828-03.

Danalet, Antonin et al. (Mar. 2016). "Location choice with longitudinal WiFi data." In: *Journal of Choice Modelling* 18, pp. 1–17. ISSN: 1755-5345. DOI: 10.1016/J.JOCM.2016.04.003.

Deb, Shuchisnigdha et al. (Sept. 2017). "Evaluating pedestrian behavior at crosswalks: Validation of a pedestrian behavior questionnaire for the U.S. population." In: *Accident Analysis & Prevention* 106, pp. 191–201. ISSN: 0001-4575. DOI: 10.1016/J.AAP.2017.05.020.

Den Heuvel, Jeroen van et al. (2015). "Using bluetooth to estimate the impact of congestion on pedestrian route choice at train stations." In: *Traffic and Granular Flow, 2013*, pp. 73–82. DOI: 10.1007/978-3-319-10629-8_9/COVER. URL: https://link.springer.com/chapter/10.1007/978-3-319-10629-8_9.

Depatla, Saandeep and Yasamin Mostofi (Oct. 2020). "Passive Crowd Speed Estimation in Adjacent Regions with Minimal WiFi Sensing." In: *IEEE Transactions on Mobile Computing* 19 (10), pp. 2429–2444. ISSN: 15580660. DOI: 10.1109/TMC.2019.2924629.

DFRobot (2023). *Most Powerful x86 Single Board Computer (SBC) LattePanda - DFRobot page 1*. URL: https://www.dfrobot.com/topic-278.html.

Dimitrova, Desislava C., Islam Alyafawi, and Torsten Braun (2012). "Experimental comparison of bluetooth and wifi signal propagation for indoor localisation." In: *Lecture Notes in Computer Science (including subseries Lecture Notes in Artificial Intelligence and Lecture Notes in Bioinformatics)* 7277 LNCS, pp. 126–137. ISSN: 03029743. DOI: 10.1007/978-3-642-30630-3_11/COVER. URL: https://link.springer.com/chapter/10.1007/978-3-642-30630-3_11.

Do, Truong, Milad Haghani, and Majid Sarvi (Jan. 2016). "Group and Single Pedestrian Behavior in Crowd Dynamics." In: *https://doi.org/10.3141/2540-02* 2540, pp. 13–19. ISSN: 03611981. DOI: 10.3141/2540-02. URL: https://journals.sagepub.com/doi/10.3141/2540-02.

Domeneghini, Jennifer, Janaina Macke, and João Alberto Rubim Sarate (2022). "Walkability Drivers for Sustainable Cities: a Pedestrian Behavior Survey." In: *Journal of Sustainable Architecture and Civil Engineering* 30 (1), pp. 65–77. ISSN: 23352000. DOI: 10.5755/J01.SACE.30.1.29756.

Domingo-Ferrer, Josep and Alberto Blanco-Justicia (2020). "Privacy-Preserving Technologies." In: *International Library of Ethics, Law and Technology* 21, pp. 279–297. ISSN: 18750036. DOI: 10.1007/978-3-030-29053-5_14/COVER. URL: https://link.springer.com/chapter/10.1007/978-3-030-29053-5_14.

Domingo-Ferrer, Josep and Krishnamurty Muralidhar (Apr. 2016). "New directions in anonymization: Permutation paradigm, verifiability by subjects and intruders, transparency to users." In: *Information Sciences* 337-338, pp. 11–24. ISSN: 00200255.

DOI: 10.1016/j.ins.2015.12.014. URL: https://linkinghub.elsevier.com/retrieve/pii/S0020025515009032.

Domingo-Ferrer, Josep, Universitat Rovira, and Virgili Vicenç Torra (2001). "Disclosure Control Methods and Information Loss for Microdata." In: ed. by Pat Doyle. Vol. 1. Elsevier, pp. 91–110.

Domingo-Ferrer, Josep, David Sánchez, and Jordi Soria-Comas (2016). "Beyond k-Anonymity: l-Diversity and t-Closeness." In: Springer, Cham, pp. 47–51. ISBN: 978-3-031-02347-7. DOI: 10.1007/978-3-031-02347-7_6. URL: https://link.springer.com/10.1007/978-3-031-02347-7_6.

Draghici, Adriana and Maarten Van Steen (Feb. 2018). "A survey of techniques for automatically sensing the behavior of a crowd." In: *ACM Computing Surveys* 51 (1). ISSN: 15577341. DOI: 10.1145/3129343.

*DS3231 RTC Module for Raspberry Pi* (n.d.). URL: https://www.cytron.io/p-ds3231-rtc-module-for-raspberry-pi.

Duives, Dorine, Winnie Daamen, and Serge Hoogendoorn (Jan. 2014a). "Influence of Group Size and Group Composition on the Adhered Distance Headway." In: *Transportation Research Procedia* 2, pp. 183–188. ISSN: 2352-1465. DOI: 10.1016/J.TRPRO.2014.09.026.

Duives, Dorine C., Winnie Daamen, and Serge Hoogendoorn (2014b). "Trajectory Analysis of Pedestrian Crowd Movements at a Dutch Music Festival." In: *Pedestrian and Evacuation Dynamics 2012*, pp. 151–166. DOI: 10.1007/978-3-319-02447-9_11. URL: https://link.springer.com/chapter/10.1007/978-3-319-02447-9_11.

Dwork, Cynthia (2011). "Differential Privacy." In: *Encyclopedia of Cryptography and Security*, pp. 338–340. DOI: 10.1007/978-1-4419-5906-5_752. URL: https://link.springer.com/referenceworkentry/10.1007/978-1-4419-5906-5_752.

Díaz, Emilio Moyano (Dec. 1997). "Teoría del comportamiento planificado e intención de infringir normas de transito en peatones." In: *Estudos de Psicologia (Natal)* 2 (2), pp. 335–348. ISSN: 1678-4669. DOI: 10.1590/S1413-294X1997000200008. URL: https://www.scielo.br/j/epsic/a/btQsMpdHX4YDztxrZCyFDBf/?lang=es.

Daz, Emilio Moyano (Sept. 2002a). "Theory of planned behavior and pedestrians' intentions to violate traffic regulations." In: *Transportation Research Part F: Traffic Psychology and Behaviour* 5 (3), pp. 169–175. ISSN: 13698478. DOI: 10.1016/S1369-8478(02)00015-3. URL: https://linkinghub.elsevier.com/retrieve/pii/S1369847802000153.

— (Sept. 2002b). "Theory of planned behavior and pedestrians' intentions to violate traffic regulations." In: *Transportation Research Part F: Traffic Psychology and Behaviour* 5 (3), pp. 169–175. ISSN: 13698478. DOI: 10.1016/S1369-8478(02)00015-3. URL: https://linkinghub.elsevier.com/retrieve/pii/S1369847802000153.

Elliott, Mark A. and Christopher J. Baughan (Nov. 2004). "Developing a self-report method for investigating adolescent road user behaviour." In: *Transportation Research Part F: Traffic Psychology and Behaviour* 7 (6), pp. 373–393. ISSN: 1369-8478. DOI: 10.1016/J.TRF.2004.10.002.

enclosure (n.d.). *Waterproof IP65 Electronic Junction Box, ABS Plastic Electrical Project Junction Enclosure Box, with Screwdriver - 200 * 120 * 75mm/White : Amazon.co.uk: DIY & Tools*. URL: https://www.amazon.co.uk/Waterproof-Electronic-Electrical-Enclosure-Screwdriver/dp/B091BYNKRF/ref=sr_1_28?crid=2HLCJ4HG7TM3N&dib=eyJ2IjoiMSJ9.o6jqEiqg3ZDy5qgOlT4xyrRQsO2HcVXHpP3-cffDAf0Tql0ZVrkDKg8JA5Nynxw5YhGT2S0N_4qgzYkCurR1Q9wa4oWVCAfA79E3Waz79QcUmmUkL8HE1R93vc

l7BLmwEUGNf2ORRGLyoZ-32i65ZHuzjkLcCpJRYE2FEWKQD1kzh_Q92jw8CHPe-o7b3GJhwvoAoYKVQUHX dC-K8.qPmp7DwrZErVOqY2J9GItK98zCh12aTsc4O1RU6gb_A&dib_tag=se&keywords=weatherproof%2Benclosure&qid=1724357816&sprefix=wetherproof%2Bencl%2Caps%2C88&sr=8-28&th=1.

Faragher, Ramsey and Robert Harle (Nov. 2015). "Location fingerprinting with bluetooth low energy beacons." In: *IEEE Journal on Selected Areas in Communications* 33 (11), pp. 2418–2428. ISSN: 07338716. DOI: 10.1109/JSAC.2015.2430281.

Farnell (2023). *Farnell Ireland - Electronic Components Distributor*. URL: https://ie.farnell.com/.

Favaretto, Rodolfo Migon, Leandro Lorenzett Dihl, and Soraia Raupp Musse (Jan. 2017). "Detecting crowd features in video sequences." In: *Proceedings - 2016 29th SIBGRAPI Conference on Graphics, Patterns and Images, SIBGRAPI 2016*, pp. 201–208. DOI: 10.1109/SIBGRAPI.2016.036.

Flueratoru, Laura et al. (Mar. 2022). "On the High Fluctuations of Received Signal Strength Measurements with BLE Signals for Contact Tracing and Proximity Detection." In: *IEEE Sensors Journal* 22 (6), pp. 5086–5100. ISSN: 15581748. DOI: 10.1109/JSEN.2021.3095710.

Foundation, OpenJS (n.d.[a]). *Node.js Run JavaScript Everywhere*. URL: https://nodejs.org/en.

Foundation, Raspberry Pi (n.d.[b]). *Raspberry Pi OS Raspberry Pi*. URL: https://www.raspberrypi.com/software/.

Fujimura, K. et al. (2011). "Behavior understandings based on state transition of postures and locations at railway station." In: *2011 IEEE International Conference on Systems, Man, and Cybernetics*, pp. 91–96. DOI: 10.1109/ICSMC.2011.6083648.

Ge, Weina, Robert T. Collins, and R. Barry Ruback (2012). "Vision-based analysis of small groups in pedestrian crowds." In: *IEEE Transactions on Pattern Analysis and Machine Intelligence* 34 (5), pp. 1003–1016. ISSN: 01628828. DOI: 10.1109/TPAMI.2011.176.

Gentry, Craig (Sept. 2009). "A Fully Homomorphic Encryption Scheme." In.

Geraghty, Tim (n.d.). "Posthoc Analysis: Tukeys Honestly Significant Difference (HSD) Test." In: (). URL: https://stats.libretexts.org/Bookshelves/Introductory_Statistics/Inferential_Statistics_and_Probability_-_A_Holistic_Approach_(Geraghty)/13\%3A_One_Factor_Analysis_of_Variance_(ANOVA)/13.06\%3A_Posthoc_Analysis__Tukeys_Honestly_Significant_Difference_(HSD)_Test85.

Gioia, Ciro et al. (Dec. 2019). "On cleaning strategies for WiFi positioning to monitor dynamic crowds." In: *Applied Geomatics* 11 (4), pp. 381–399. ISSN: 1866928X. DOI: 10.1007/S12518-019-00260-Z/FIGURES/16. URL: https://link.springer.com/article/10.1007/s12518-019-00260-z.

*GPS Logger - Apps on Google Play* (n.d.). URL: https://play.google.com/store/apps/details?id=com.peterhohsy.gpsloggerlite.

Granié, Marie-Axelle, Marjorie Pannetier, and Ludivine Guého (2013). "Developing a self-reporting method to measure pedestrian behaviors at all ages." In: *Accident Analysis and Prevention* 50, pp. 830–839. DOI: 10.1016/j.aap.2012.07.009. URL: http://dx.doi.org/10.1016/j.aap.2012.07.009.

Guillen-Perez, Antonio and Maria-Dolores Cano (2021). "Pedestrian characterisation in urban environments combining WiFi and AI." English. In: *INTERNATIONAL JOURNAL OF SENSOR NETWORKS* 37.1, pp. 48–60. ISSN: 1748-1279. DOI: 10.1504/IJSNET.2021.117964.

Hackshaw, Allan and Amy Kirkwood (July 2024). "Origin of the 5% p-value threshold." In: *BMJ* 343 (7815). ISSN: 17561833. DOI: 10.1136/BMJ.D3340.

Haghani, Ali et al. (Jan. 2010). "Data Collection of Freeway Travel Time Ground Truth with Bluetooth Sensors." In: *Transportation Research Record: Journal of the Transportation Research Board* 2160 (1), pp. 60–68. ISSN: 0361-1981. DOI: 10.3141/2160-07. URL: http://journals.sagepub.com/doi/10.3141/2160-07.

Hahm, Yeankyoung, Heeyeun Yoon, and Yunwon Choi (June 2019). "The effect of built environments on the walking and shopping behaviors of pedestrians; A study with GPS experiment in Sinchon retail district in Seoul, South Korea." In: *Cities* 89, pp. 1–13. ISSN: 0264-2751. DOI: 10.1016/J.CITIES.2019.01.020.

Haklay, Mordechai and Patrick Weber (2008). "OpenStreetMap: User-Generated Street Maps." In: *IEEE Pervasive Computing* 7.4, pp. 12–18. DOI: 10.1109/MPRV.2008.80.

Han, Kyuwon et al. (2021). "Exploiting User Mobility for WiFi RTT Positioning: A Geometric Approach." In: *IEEE INTERNET OF THINGS JOURNAL* 8.19, pp. 14589–14606. ISSN: 2327-4662. DOI: 10.1109/JIOT.2021.3070367.

Hill, Michael R. (Sept. 1984). "Stalking the Urban Pedestrian." In: *Environment and Behavior* 16 (5), pp. 539–550. ISSN: 1552390X. DOI: 10.1177/0013916584165001.

Huang, Baoqi et al. (2021). "Pedestrian Flow Estimation Through Passive WiFi Sensing." In: *IEEE TRANSACTIONS ON MOBILE COMPUTING* 20.4, pp. 1529–1542. ISSN: 1536-1233. DOI: 10.1109/TMC.2019.2959610.

*IanHarvey/bluepy* (n.d.). URL: https://github.com/IanHarvey/bluepy.

*InfluxDB Time Series Data Platform | InfluxData* (n.d.). URL: https://www.influxdata.com/.

Kasemsuppakorn, Piyawan and Hassan A. Karimi (Jan. 2013a). "A pedestrian network construction algorithm based on multiple GPS traces." In: *Transportation Research Part C: Emerging Technologies* 26, pp. 285–300. ISSN: 0968-090X. DOI: 10.1016/J.TRC.2012.09.007.

— (Jan. 2013b). "Pedestrian Path Generation through GPS Traces." In: *Advanced Location-Based Technologies and Services*, pp. 165–185. DOI: 10.1201/B14940-9/PEDESTRIAN-PATH-GENERATION-GPS-TRACES-PIYAWAN-KASEMSUPPAKORN-HASSAN-KARIMI. URL: https://www.taylorfrancis.com/chapters/oa-edit/10.1201/b14940-9/pedestrian-path-generation-gps-traces-piyawan-kasemsuppakorn-hassan-karimi.

Khan, Muhammad Imran and Simon N Foley (2021). "From k-anonymity to Differential Privacy: A Brief Introduction to Formal Privacy Models." In: URL: https://hal.science/hal-03226881.

Kitazato, Tomoya, Masaki Ito, and Kaoru Sezaki (Oct. 2018). "A Study of the Detection of Pedestrian Flow Using Bluetooth Low Energy." In: *2018 IEEE International Conference on Pervasive Computing and Communications Workshops, PerCom Workshops 2018*, pp. 716–721. DOI: 10.1109/PERCOMW.2018.8480336.

Koledoye, Moses A. et al. (Oct. 2018). "A Comparison of RSSI Filtering Techniques for Range-based Localization." In: *IEEE International Conference on Emerging Technologies and Factory Automation, ETFA* 2018-September, pp. 761–767. ISSN: 19460759. DOI: 10.1109/ETFA.2018.8502556.

Krchák, Martin et al. (2024). "Advancements in Antenna Measurement." In: 1108. DOI: 10.1007/978-3-031-48835-1. URL: https://link.springer.com/10.1007/978-3-031-48835-1.

Kristoffersen, Miklas S. et al. (Jan. 2016). "Pedestrian Counting with Occlusion Handling Using Stereo Thermal Cameras." In: *Sensors 2016, Vol. 16, Page 62* 16 (1), p. 62. ISSN: 1424-8220. DOI: 10.3390/S16010062. URL: https://www.mdpi.com/1424-8220/16/1/62/htmhttps://www.mdpi.com/1424-8220/16/1/62.

Kumar, Santosh et al. (Aug. 2018). "An intelligent decision computing paradigm for crowd monitoring in the smart city." In: *Journal of Parallel and Distributed Computing* 118, pp. 344–358. ISSN: 0743-7315. DOI: 10.1016/J.JPDC.2017.03.002.

Kunchala, Anil, Melanie Bouroche, and Bianca Schoen-Phelan (2023). "Towards A Framework for Privacy-Preserving Pedestrian Analysis." In: *Proceedings - 2023 IEEE Winter Conference on Applications of Computer Vision, WACV 2023*, pp. 4359–4369. DOI: 10.1109/WACV56688.2023.00435.

Lam, Hing Keung William, John F. Morrall, and Herbert Ho (July 1995). "Pedestrian flow characteristics in Hong Kong." In: *Transportation Research Record* (1487), pp. 56–62. ISSN: 0361-1981.

Larroya, Ferran et al. (July 2023). "Home-to-school pedestrian mobility GPS data from a citizen science experiment in the Barcelona area." In: *Scientific Data 2023 10:1* 10 (1), pp. 1–17. ISSN: 2052-4463. DOI: 10.1038/s41597-023-02328-3. URL: https://www.nature.com/articles/s41597-023-02328-3.

Lerner, Alon et al. (2009). "Fitting behaviors to pedestrian simulations." In: pp. 199–208. DOI: 10.1145/1599470.1599496.

Leutenegger, Stefan, Margarita Chli, and Roland Y. Siegwart (2011). "BRISK: Binary Robust invariant scalable keypoints." In: *Proceedings of the IEEE International Conference on Computer Vision*, pp. 2548–2555. DOI: 10.1109/ICCV.2011.6126542.

Li, Ninghui, Tiancheng Li, and Suresh Venkatasubramanian (Apr. 2007). "t-Closeness: Privacy Beyond k-Anonymity and l-Diversity." In: IEEE, pp. 106–115. ISBN: 1-4244-0802-4. DOI: 10.1109/ICDE.2007.367856. URL: https://ieeexplore.ieee.org/document/4221659/.

Li, Xing et al. (Sept. 2015). "A (Leveled) fully homomorphic encryption scheme based on error-free approximate GCD." In: *ICEIEC 2015 - Proceedings of 2015 IEEE 5th International Conference on Electronics Information and Emergency Communication*, pp. 224–227. DOI: 10.1109/ICEIEC.2015.7284526.

Li, Xun et al. (June 2022). "Towards Building a Visual Behaviour Analysis Pipeline for Suicide Detection and Prevention." In: *Sensors 2022, Vol. 22, Page 4488* 22 (12), p. 4488. ISSN: 1424-8220. DOI: 10.3390/S22124488. URL: https://www.mdpi.com/1424-8220/22/12/4488/htmhttps://www.mdpi.com/1424-8220/22/12/4488.

Liao, Samuel Y. (1990). *Microwave Devices and Circuits*. 3rd. Englewood Cliffs, NJ: Prentice Hall. ISBN: 978-0135832042.

Liao, Weichen et al. (Jan. 2014). "Experimental Study on Pedestrian Flow through Wide Bottleneck." In: *Transportation Research Procedia* 2, pp. 26–33. ISSN: 2352-1465. DOI: 10.1016/J.TRPRO.2014.09.005.

Little, R (1993). "Statistical Analysis of Masked Data." In: *Journal of Official Statistics* 9 (2), pp. 407–426.

Liu, Jialai et al. (2022). "Toward robust and adaptive pedestrian monitoring using CSI: design, implementation, and evaluation." In: *NEURAL COMPUTING & APPLICATIONS* 34.14, SI, pp. 12063–12075. ISSN: 0941-0643. DOI: 10.1007/s00521-022-07094-8.

Livi, A., K. Clifton, and G. Martin (2004). "ISSUES AND METHODS IN CAPTURING PEDESTRIAN BEHAVIORS, ATTITUDES AND PERCEPTIONS: EXPERIENCES WITH A COMMUNITY-BASED WALKABILITY SURVEY." In.

Lue, Gregory and Eric J. Miller (Jan. 2019). "Estimating a Toronto pedestrian route choice model using smartphone GPS data." In: *Travel Behaviour and Society* 14, pp. 34–42. ISSN: 2214-367X. DOI: 10.1016/J.TBS.2018.09.008.

Maheshwari, Tanvi et al. (2016). "Virtual Reality as a tool to assess perception of safety and comfort for cyclists in Singapore." In.

Martani, Claudio et al. (June 2017). "Pedestrian monitoring techniques for crowd-flow prediction." In: *Proceedings of the Institution of Civil Engineers - Smart Infrastructure and Construction* 170 (2), pp. 17–27. DOI: 10.1680/JSMIC.17.00001.

McArdle, Gavin et al. (2014). "Classifying pedestrian movement behaviour from GPS trajectories using visualization and clustering." In: *Annals of GIS* 20 (2), pp. 85–98. ISSN: 19475691. DOI: 10.1080/19475683.2014.904560. URL: https://www.tandfonline.com/doi/abs/10.1080/19475683.2014.904560.

Medileh, Saci et al. (Apr. 2023). "A Multi-Key with Partially Homomorphic Encryption Scheme for Low-End Devices Ensuring Data Integrity." In: *Information 2023, Vol. 14, Page 263* 14 (5), p. 263. ISSN: 2078-2489. DOI: 10.3390/INFO14050263. URL: https://www.mdpi.com/2078-2489/14/5/263/htmhttps://www.mdpi.com/2078-2489/14/5/263.

*Micro:bit Educational Foundation | micro:bit* (n.d.). URL: https://microbit.org/.

Molisch, Andreas F. (2012). *Wireless Communications*. John Wiley & Sons, p. 884. ISBN: 1118355687. URL: https://books.google.com/books/about/Wireless_Communications.html?id=877tFGeQo5oC.

Montanari, Alessandro et al. (May 2017). "A Study of Bluetooth Low Energy performance for human proximity detection in the workplace." In: *2017 IEEE International Conference on Pervasive Computing and Communications, PerCom 2017*, pp. 90–99. DOI: 10.1109/PERCOM.2017.7917855.

MontAlvão, Claudia, Carolina Esteves, and Mariana Dias (2021). "Aspects of Brazilian Pedestrian Behavior: A Questionnaire Study." In: *Lecture Notes in Networks and Systems* 221 LNNS, pp. 751–756. ISSN: 23673389. DOI: 10.1007/978-3-030-74608-7_92/COVER. URL: https://link.springer.com/chapter/10.1007/978-3-030-74608-7_92.

Moussaïd, Mehdi et al. (2010). "The Walking Behaviour of Pedestrian Social Groups and Its Impact on Crowd Dynamics." In: *PLOS ONE* 5 (4), e10047. ISSN: 1932-6203. DOI: 10.1371/JOURNAL.PONE.0010047. URL: https://journals.plos.org/plosone/article?id=10.1371/journal.pone.0010047.

Moussaïd, Mehdi et al. (Sept. 2016). "Crowd behaviour during high-stress evacuations in an immersive virtual environment." In: *Journal of The Royal Society Interface* 13 (122). ISSN: 17425662. DOI: 10.1098/RSIF.2016.0414. URL: https://royalsocietypublishing.org/doi/10.1098/rsif.2016.0414.

Natapov, A. and D. Fisher-Gewirtzman (July 2016). "Visibility of urban activities and pedestrian routes: An experiment in a virtual environment." In: *Computers, Environment and Urban Systems* 58, pp. 60–70. ISSN: 0198-9715. DOI: 10.1016/J.COMPENVURBSYS.2016.03.007.

Parmar, Mayank, Paula Kelly, and Damon Berry (2022). "Effects of Body Occlusion on Bluetooth Low Energy RSSI in Identifying Close Proximity of Pedestrians in Outdoor Environments." In: *ISC2 2022 - 8th IEEE International Smart Cities Conference*. DOI: 10.1109/ISC255366.2022.9922048.

— (Sept. 2023a). "Detection of Pause in a Pedestrian's Movement on a Linear Walkway using Bluetooth Low Energy Received Signal Strength Indicator." In: IEEE, pp. 1–7. ISBN: 979-8-3503-9775-8. DOI: 10.1109/ISC257844.2023.10293694. URL: https://ieeexplore.ieee.org/document/10293694/.

— (Sept. 2023b). "Indication of Pedestrian's Travel Direction Through Bluetooth Low Energy Signals Perceived by a Single Observer Device." In: IEEE, pp. 1–7. ISBN: 979-8-3503-9775-8. DOI: 10.1109/ISC257844.2023.10293305. URL: https://ieeexplore.ieee.org/document/10293305/.

PE, Jason S Wasson, James R Sturdevant PE, and Darcy M Bullock PE (June 2008). "Real-Time Travel Time Estimates Using Media Access Control Address Matching." In: *Institute of Transportation Engineers. ITE Journal* 78 (6). Copyright - Copyright Institute of Transportation Engineers Jun 2008 Document feature - References; Maps; Graphs; Tables; Photographs Last updated - 2023-11-25 CODEN - ITEJDZ SubjectsTermNotLitGenreText - United States–US, pp. 20–23. ISSN: 01628178. URL: https://tudublin.idm.oclc.org/login?url=https://www.proquest.com/scholarly-journals/real-time-travel-estimates-using-media-access/docview/224879455/se-2?accountid=10594.

Peng, Yu Li et al. (2013). "Propagation Characteristics of 2.4 GHz Wireless Channel at Different Directions and Heights in Tea Plantation." In: *Applied Mechanics and Materials* 325-326, pp. 1697–1701. ISSN: 1662-7482. DOI: 10.4028/WWW.SCIENTIFIC.NET/AMM.325-326.1697. URL: https://www.scientific.net/AMM.325-326.1697.

Piccoli, B. and A. Tosin (2008). "Time-Evolving Measures and Macroscopic Modeling of Pedestrian Flow." In: *Archive for Rational Mechanics and Analysis* 199, pp. 707–738. DOI: 10.1007/s00205-010-0366-y.

Privacy, IEEE Digital (2023). *What Is Differential Privacy? - IEEE Digital Privacy*. URL: https://digitalprivacy.ieee.org/publications/topics/what-is-differential-privacy.

Project, The Debian (n.d.). *Debian – The Universal Operating System*. URL: https://www.debian.org/.

Qi, Xinjun and Mingkui Zong (Jan. 2012). "An Overview of Privacy Preserving Data Mining." In: *Procedia Environmental Sciences* 12, pp. 1341–1347. ISSN: 1878-0296. DOI: 10.1016/J.PROENV.2012.01.432.

Qureshi, F. and Demetri Terzopoulos (2005). "Surveillance camera scheduling: a virtual vision approach." In: *Multimedia Systems* 12, pp. 269–283. DOI: 10.1007/s00530-006-0059-4.

Rappaport, Theodore S. (2002). *Wireless Communications: Principles and Practice*. 2nd ed. Prentice Hall.

RaspberryPi-Foundation (2023). *Raspberry Pi*. URL: https://www.raspberrypi.com/.

Reason, James et al. (1990). "Errors and violations on the roads: a real distinction?" In: *ERGONOMICS* 33 (10-11), pp. 1315–1332. ISSN: 13665847. DOI: 10.1080/00140139008925335.

Rivest, R. L., A. Shamir, and L. Adleman (1978). "A Method for Obtaining Digital Signatures and Public-Key Cryptosystems." In: *Commun. ACM* 21.2, pp. 120126. ISSN: 0001-0782. DOI: 10.1145/359340.359342. URL: https://doi.org/10.1145/359340.359342.

Rubin, D (1993). "Statistical Disclosure Limitation." In: *Journal of Official Statistics* 9 (2), pp. 461–468.

Ruuvi (n.d.). *RuuviTag Wireless Sensor - Ruuvi*. URL: https://ruuvi.com/ruuvitag/.

Sawas, Abdullah M. et al. (2018). "Trajectolizer: Interactive Analysis and Exploration of Trajectory Group Dynamics." In: *2018 19th IEEE International Conference on Mobile Data Management (MDM)*, pp. 286–287. DOI: 10.1109/MDM.2018.00053.

Schauer, Lorenz, Martin Werner, and Philipp Marcus (2014). "Estimating crowd densities and pedestrian flows using Wi-Fi and bluetooth." In: *MobiQuitous 2014 - 11th International Conference on Mobile and Ubiquitous Systems: Computing, Networking and Services*, pp. 171–177. DOI: 10.4108/ICST.MOBIQUITOUS.2014.257870. URL: https://dl.acm.org/doi/10.4108/icst.mobiquitous.2014.257870.

Seyfried, Armin et al. (Oct. 2005). "The fundamental diagram of pedestrian movement revisited." In: *Journal of Statistical Mechanics: Theory and Experiment* 2005 (10), P10002. ISSN: 1742-5468. DOI: 10.1088/1742-5468/2005/10/P10002. URL: https://iopscience.iop.org/article/10.1088/1742-5468/2005/10/P10002https://iopscience.iop.org/article/10.1088/1742-5468/2005/10/P10002/meta.

Shah, Jiten, G.J. Joshi, and Purnima Parida (Dec. 2013). "Behavioral Characteristics of Pedestrian Flow on Stairway at Railway Station." In: *Procedia - Social and Behavioral Sciences* 104, pp. 688–697. ISSN: 1877-0428. DOI: 10.1016/J.SBSPRO.2013.11.163.

Shenoi, B. A. (2006). *Introduction to Digital Signal Processing and Filter Design*. John Wiley & Sons, Inc. ISBN: 9780471464822. DOI: 10.1002/0471656372.

Sig, Bluetooth (2014). *Specification of the Bluetooth System: Volume 6, Part B*. URL: https://www.bluetooth.org/en-us/specification/adopted-specifications.

Spek, Stefan van der (Sept. 2008). "Spatial Metro: Tracking pedestrians in historic city centres." In: *Research in Urbanism Series* 1. gps, tracking, experience of the users of public space<br/>, pp. 77–97. ISSN: 1879-8217. DOI: 10.7480/RIUS.1.198. URL: https://www.rius.ac/index.php/rius/article/view/59.

Su, Bing et al. (Feb. 2023). "K-Anonymity Privacy Protection Algorithm for Multi-Dimensional Data against Skewness and Similarity Attacks." In: *Sensors (Basel, Switzerland)* 23 (3). ISSN: 14248220. DOI: 10.3390/S23031554. URL: /pmc/articles/PMC9919945//pmc/articles/PMC9919945/?report=abstracthttps://www.ncbi.nlm.nih.gov/pmc/articles/PMC9919945/.

Tan, Amy A.W., Bauke de Vries, and Harry J.P. Timmermans (Aug. 2006). "Using a Stereo Panoramic Interactive Navigation System to Measure Pedestrian Activity Scheduling Behaviour: A Test of Validity." In: *https://doi.org/10.1068/b31092* 33 (4), pp. 541–557. ISSN: 02658135. DOI: 10.1068/B31092. URL: https://journals.sagepub.com/doi/10.1068/b31092.

Tanaboriboon, Yordphol, Sim Siang Hwa, and Chin Hoong Chor (May 1986). "Pedestrian Characteristics Study in Singapore." In: *Journal of Transportation Engineering* 112 (3), pp. 229–235. ISSN: 0733947X. DOI: 10.1061/(ASCE)0733-947X(1986)112:3(229). URL: https://ascelibrary.org/doi/abs/10.1061/%28ASCE%290733-947X%281986%29112%3A3%28229%29https://ascelibrary.org/doi/10.1061/%28ASCE%290733-947X%281986%29112%3A3%28229%29.

Tang, Chieh Hsin, Wu Tai Wu, and Ching Yuan Lin (July 2009). "Using virtual reality to determine how emergency signs facilitate way-finding." In: *Applied Ergonomics* 40 (4), pp. 722–730. ISSN: 0003-6870. DOI: 10.1016/J.APERGO.2008.06.009.

Taub, J, M Elliot, and J W Sakshaug (2020). "The Impact of Synthetic Data Generation on Data Utility with Application to the 1991 UK Samples of Anonymised Records." In: *Transactions on Data Privacy* 13 (1), pp. 1–23. URL: http://www.tdp.cat/issues16/abs.a306a18.php.

Ton, Danique et al. (2015). "Route and activity location choice behaviour of departing passengers in train stations." In: *hEART (European Association for Research in Transportation)*.

Torra, Vicenç (2022). "Disclosure, Privacy Models, and Privacy Mechanisms." In: pp. 53–106. ISSN: 2197-1781. DOI: 10.1007/978-3-031-12837-0_3. URL: https://link.springer.com/chapter/10.1007/978-3-031-12837-0_3.

Torre, Damiano, Anitha Chennamaneni, and Alex Rodriguez (2023). "Privacy-Preservation Techniques for IoT Devices: A Systematic Mapping Study." In: *IEEE Access* 11, pp. 16323–16345. ISSN: 2169-3536. DOI: 10.1109/ACCESS.2023.3245524. URL: https://ieeexplore.ieee.org/document/10044661/.

Vandroux, Romane et al. (Feb. 2022). "The pedestrian behaviour scale: A systematic review of its validation around the world." In: *Accident Analysis & Prevention* 165, p. 106509. ISSN: 0001-4575. DOI: 10.1016/J.AAP.2021.106509.

Vilar, Elisângela, Francisco Rebelo, and Paulo Noriega (Nov. 2014). "Indoor Human Wayfinding Performance Using Vertical and Horizontal Signage in Virtual Reality." In: *Human Factors and Ergonomics in Manufacturing & Service Industries* 24 (6), pp. 601–615. ISSN: 1520-6564. DOI: 10.1002/HFM.20503. URL: https://onlinelibrary.wiley.com/doi/full/10.1002/hfm.20503https://onlinelibrary.wiley.com/doi/abs/10.1002/hfm.20503https://onlinelibrary.wiley.com/doi/10.1002/hfm.20503.

Virkler, M. and Sathish Elayadath (1994). "PEDESTRIAN SPEED-FLOW-DENSITY RELATIONSHIPS." In: *Transportation Research Record*.

Wang, Tingli (2023). "Study on the Simulation and Optimization of Pedestrian Flow in Metro Stations Based on Anylogic." In: *Advances in Computer, Signals and Systems*. DOI: 10.23977/acss.2023.070907.

Wilcox, Rand R. (Jan. 2021). "Introduction to Robust Estimation and Hypothesis Testing." In: *Introduction to Robust Estimation and Hypothesis Testing*, pp. 1–900. DOI: 10.1016/C2019-0-01225-3.

Winer, B.J., D.R. Brown, and K.M. Michels (1991). *Statistical Principles in Experimental Design*. 3rd. New York: McGraw-Hill. ISBN: 978-0070709827.

Xu, Weijia et al. (2018). "Automated pedestrian safety analysis using data from traffic monitoring cameras." In: *Proceedings of the 1st ACM/EIGSCC Symposium on Smart Cities and Communities*. DOI: 10.1145/3236461.3241972.

Yao, Andrew Chi Chih (1986). "HOW TO GENERATE AND EXCHANGE SECRETS." In: *Annual Symposium on Foundations of Computer Science (Proceedings)*, pp. 162–167. ISSN: 02725428. DOI: 10.1109/SFCS.1986.25.

Yoshimura, Yuji et al. (Apr. 2017). "Analysis of pedestrian behaviors through non-invasive Bluetooth monitoring." In: *Applied Geography* 81, pp. 43–51. ISSN: 0143-6228. DOI: 10.1016/J.APGEOG.2017.02.002.

Zaiontz, Charles (n.d.). "Tukey HSD (Honestly Significant Difference)." In: Accessed: 2024-07-15. URL: https://real-statistics.com/one-way-analysis-of-variance-anova/unplanned-comparisons/tukey-hsd/.

Zhang, Jun and Armin Seyfried (Jan. 2014). "Quantification of Bottleneck Effects for Different Types of Facilities." In: *Transportation Research Procedia* 2, pp. 51–59. ISSN: 2352-1465. DOI: 10.1016/J.TRPRO.2014.09.008.

Zhao, Jondy (2023). *pyarmor ů PyPI*. URL: https://pypi.org/project/pyarmor/.

Éireann, Met (2023). *Phoenix Park Hourly Data*. Accessed: January 18, 2025. URL: https://data.gov.ie/dataset/phoenix-park-hourly-data/resource/b7153609-7361-472a-b6fd-e3c1b957c565.